



Calhoun: The NPS Institutional Archive
DSpace Repository

Theses and Dissertations

1. Thesis and Dissertation Collection, all items

1992-03

Comparison of electromagnetic propagation predictions from IREPS and RPO across a coastal transition

Campbell, Bryce; Siletzky, Stephan

Monterey, California. Naval Postgraduate School

<https://hdl.handle.net/10945/38547>

This publication is a work of the U.S. Government as defined in Title 17, United States Code, Section 101. Copyright protection is not available for this work in the United States.

Downloaded from NPS Archive: Calhoun



Calhoun is the Naval Postgraduate School's public access digital repository for research materials and institutional publications created by the NPS community. Calhoun is named for Professor of Mathematics Guy K. Calhoun, NPS's first appointed -- and published -- scholarly author.

Dudley Knox Library / Naval Postgraduate School
411 Dyer Road / 1 University Circle
Monterey, California USA 93943

<http://www.nps.edu/library>

2

NAVAL POSTGRADUATE SCHOOL Monterey, California

AD-A249 331



DTIC
SELECTE
APR 24 1992
S B D

THESIS

Comparison of Electromagnetic Propagation Predictions
From IREPS and RPO Across a Coastal Transition

by

Bryce Campbell
and
Stephan Siletzky

March, 1992

Thesis Advisor:

John W. Glendening

Approved for public release; distribution is unlimited.

92-10523



02 4 23 038

| REPORT DOCUMENTATION PAGE | | | | Form Approved OMB No. 0704-0188 | |
|---|---|--|-------------------|------------------------------------|------------------------|
| 1a REPORT SECURITY CLASSIFICATION | | 1b RESTRICTIVE MARKINGS | | | |
| 2a SECURITY CLASSIFICATION AUTHORITY | | 3. DISTRIBUTION/AVAILABILITY OF REPORT Approved for public release; distribution is unlimited. | | | |
| 2b. DECLASSIFICATION/DOWNGRADING SCHEDULE | | | | | |
| 4. PERFORMING ORGANIZATION REPORT NUMBER(S) | | 5. MONITORING ORGANIZATION REPORT NUMBER(S) | | | |
| 6a NAME OF PERFORMING ORGANIZATION | 6b OFFICE SYMBOL (if applicable) | 7a. NAME OF MONITORING ORGANIZATION | | | |
| Naval Postgraduate School | 39 | Naval Postgraduate School | | | |
| 6c. ADDRESS (City, State, and ZIP Code) | | 7b ADDRESS (City, State, and ZIP Code) | | | |
| Monterey, CA 93943-5000 | | Monterey, CA 93943-5000 | | | |
| 8a. NAME OF FUNDING/SPONSORING ORGANIZATION | 8b OFFICE SYMBOL (if applicable) | 9 PROCUREMENT INSTRUMENT IDENTIFICATION NUMBER | | | |
| 8c. ADDRESS (City, State, and ZIP Code) | | 10 SOURCE OF FUNDING NUMBERS | | | |
| | | PROGRAM ELEMENT NO | PROJECT NO | TASK NO | WORK UNIT ACCESSION NO |
| 11 TITLE (Include Security Classification) COMPARISON OF ELECTROMAGNETIC PROPAGATION PREDICTIONS FROM IREPS AND RPO ACROSS A COASTAL TRANSITION | | | | | |
| 12 PERSONAL AUTHOR(S) Bryce Campbell and Stephan Siletzky | | | | | |
| 13a TYPE OF REPORT | 13b TIME COVERED FROM _____ TO _____ | 14. DATE OF REPORT (Year, Month, Day) | 15 PAGE COUNT | | |
| Master's Thesis | | 1992 March | 89 | | |
| 16 SUPPLEMENTARY NOTATION The views expressed in this thesis are those of the authors and do not reflect the official position of the Department of Defense or the U.S. Government. | | | | | |
| 17 COSATI CODES | | 18 SUBJECT TERMS (Continue on reverse if necessary and identify by block number) | | | |
| FIELD | GROUP | IREPS Littoral Warfare Coastal AAW | | | |
| | | RPO Littoral Electromagnetic Propagation | | | |
| 19 ABSTRACT (Continue on reverse if necessary and identify by block number) | | | | | |
| <p>The Navy's existing electromagnetic propagation prediction software, the Integrated Refractive Effects Prediction System (IREPS), neglects signal leakage from a duct, approximates diffraction, and assumes atmospheric horizontal homogeneity. To ameliorate these deficiencies, the Radio Physics Optics (RPO) program is being developed. This thesis analyzes the significantly different propagation predictions of the two models. RPO predicts significantly shorter propagation ranges in a duct than does IREPS. RPO predicts variations in duct thickness and height which IREPS idealizes, and RPO also computes a signal strength above the duct. Only RPO predicts significant interactions between the duct's dm/dz gradient and frequency. RPO is capable of modeling propagation paths for an inhomogeneous atmosphere. Neglecting atmospheric</p> | | | | | |
| 20 DISTRIBUTION/AVAILABILITY OF ABSTRACT | | 21 ABSTRACT SECURITY CLASSIFICATION | | | |
| <input checked="" type="checkbox"/> UNCLASSIFIED/UNLIMITED <input type="checkbox"/> SAME AS RPT <input type="checkbox"/> DTIC USERS | | UNCLASSIFIED | | | |
| 22. NAME OF RESPONSIBLE INDIVIDUAL | | 22b TELEPHONE (Include Area Code) | 22c OFFICE SYMBOL | | |
| John W. Glendening | | (408) 646-2674 | MR/Gn | | |

Item 19 Continued

inhomogeneities in a coastal region introduces significant propagation prediction errors.

Approved for public release; distribution is unlimited.

Comparison of Electromagnetic Propagation Predictions From IREPS and RPO

Across a Coastal Transition

by

Bryce Campbell

Lieutenant, United States Navy

B.S., University of Texas at El Paso, 1979

and

Stephan Siletzky

Lieutenant, United States Navy

B.S.M.E., United States Naval Academy, 1985

Submitted in partial fulfillment

of the requirements for the degree of

MASTER OF SCIENCE IN SYSTEMS TECHNOLOGY

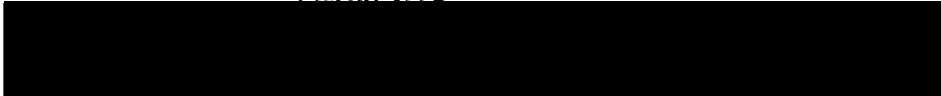
(Joint Command, Control, and Communications)

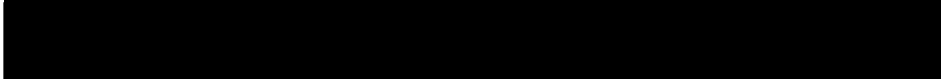
from the

NAVAL POSTGRADUATE SCHOOL

March, 1992

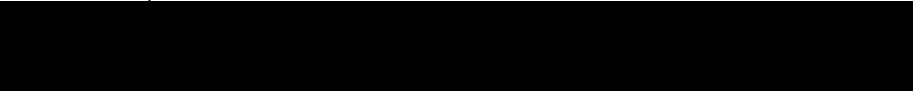
Authors:

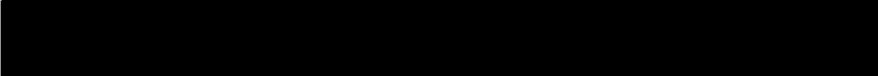

Bryce Campbell


Stephan Siletzky

Approved by:


John W. Glendening, Principal Advisor


Kenneth L. Davidson, Associate Advisor


Carl R. Jones, Chairman

Joint Command, Control, and Communications Academic Group

ABSTRACT

The Navy's existing electromagnetic propagation prediction software, the Integrated Refractive Effects Prediction System (IREPS), neglects signal leakage from a duct, approximates diffraction, and assumes atmospheric horizontal homogeneity. To ameliorate these deficiencies, the Radio Physics Optics (RPO) program is being developed. This thesis analyzes the significantly different propagation predictions of the two models. RPO predicts significantly shorter propagation ranges in a duct than does IREPS. RPO predicts variations in duct thickness and height which IREPS idealizes, and RPO also computes a signal strength above the duct. Only RPO predicts significant interactions between the duct's dm/dz gradient and frequency. RPO is capable of modeling propagation paths for an inhomogeneous atmosphere. Neglecting atmospheric inhomogeneities in a coastal region introduces significant propagation prediction errors.

| | |
|----------------------|-------------------------------------|
| Accession For | |
| NTIS GRA&I | <input checked="" type="checkbox"/> |
| DTIC TAB | <input type="checkbox"/> |
| Unannounced | <input type="checkbox"/> |
| Justification | |
| By | |
| Distribution/ | |
| Availability Codes | |
| Dist | Avail and/or Special |
| A-1 | |



TABLE OF CONTENTS

| | |
|---|----|
| I. INTRODUCTION | 1 |
| II. ATMOSPHERIC REFRACTIVITY | 4 |
| A. GENERAL | 4 |
| B. ELECTROMAGNETIC SPECTRUM | 5 |
| C. REFRACTIVITY | 5 |
| D. TRAPPING AND DUCTING | 7 |
| E. THE COASTAL ENVIRONMENT | 12 |
| F. REFRACTIVITY PREDICTION PROGRAMS | 14 |
| 1. Integrated Refractive Effects Prediction System (IREPS) | 14 |
| 2. Radio Physics Optics Program (RPO) | 17 |
| III. METEOROLOGICAL CONDITIONS AND TACTICAL ENVIRONMENT | 19 |
| A. SCENARIO | 19 |
| B. METEOROLOGICAL CONDITIONS | 21 |
| 1. Offshore | 21 |
| 2. Over Land | 24 |
| C. FREQUENCY AND ANTENNA SELECTION | 26 |
| D. SUMMARY | 27 |

| | |
|---|----|
| IV. COMPARISON AND ANALYSIS OF IREPS AND RPO RESULTS FOR | |
| A HORIZONTALLY HOMOGENEOUS ATMOSPHERE | 29 |
| A. INTRODUCTION | 29 |
| 1. General | 29 |
| 2. Output Display | 29 |
| 3. Data Collection | 30 |
| 4. Antenna Lobe Patterns | 30 |
| B. CASE 1 | 31 |
| 1. Environment | 31 |
| 2. Results for the 150 MHz Analysis | 31 |
| 3. Results for the 350 MHz Analysis | 33 |
| 4. Results for the 3 GHz Analysis | 35 |
| C. CASE 2 | 37 |
| 1. Environment | 37 |
| 2. Results for the 150 MHz Analysis | 37 |
| 3. Results for the 350 MHz Analysis | 39 |
| 4. Results for the 3 GHz Analysis | 41 |
| 5. Interaction Between Duct dM/dz Gradient and Frequency | 41 |
| D. CASE 3 | 43 |
| 1. Environment | 43 |
| 2. Results for the 150 MHz Analysis | 43 |
| 3. Results for the 350 Mhz Analysis | 45 |
| 4. Results for the 3 GHz Analysis | 45 |
| E. SUMMARY | 45 |

| | | |
|-----|---|----|
| V. | ANALYSIS OF RPO RESULTS FOR A HORIZONTALLY | |
| | INHOMOGENEOUS ATMOSPHERE | 51 |
| A. | INTRODUCTION | 51 |
| B. | CASE 1 | 52 |
| | 1. Environment | 52 |
| | 2. Results for the 150 MHz Analysis | 53 |
| | 3. Results for the 350 MHz Analysis | 53 |
| | 4. Results for the 3 GHz Analysis | 56 |
| C. | CASE 2 | 58 |
| | 1. Environment | 58 |
| | 2. Results for the 150 MHz Analysis | 58 |
| | 3. Results for the 350 MHz Analysis | 58 |
| | 4. Results for the 3 GHz Analysis | 61 |
| | 5. Interaction Between Duct dM/dz Gradient and Frequency | 61 |
| D. | CASE 3 | 61 |
| | 1. Environment | 61 |
| | 2. Summarized Results for All Frequencies | 63 |
| E. | SHORE TO SEA PERSPECTIVE (COASTAL RADAR) | 63 |
| F. | SUMMARY | 65 |
| VI. | CONCLUSIONS | 67 |
| A. | GENERAL | 67 |
| B. | ASSUMPTIONS IN TESTING | 68 |
| C. | PREDICTION DIFFERENCES BETWEEN IREPS AND RPO | 69 |

D. RPO RESULTS FOR A HORIZONTALLY INHOMOGENEOUS
COASTAL ATMOSPHERE 71

E. SUMMARY 71

LIST OF REFERENCES 72

BIBLIOGRAPHY 73

INITIAL DISTRIBUTION LIST 74

LIST OF TABLES

TABLE 3.1 CASES ANALYZED 28

LIST OF FIGURES

| | | |
|-------------------|---|----|
| Figure 2.1 | Classical ducting | 8 |
| Figure 2.2 | Determining duct thickness | 9 |
| Figure 2.3 | Duct types | 10 |
| Figure 2.4 | The coastal transition | 13 |
| Figure 3.1 | Battle group scenario | 20 |
| Figure 3.2 | M-profile for 02 NOV 89 (offshore) | 22 |
| Figure 3.3 | M-profile for 03 NOV 89 (offshore) | 22 |
| Figure 3.4 | M-profile for 05 NOV 89 (offshore) | 23 |
| Figure 3.5 | M-profile for 02 NOV 89 (over land) | 24 |
| Figure 3.6 | M-profile for 03 NOV 89 (over land) | 25 |
| Figure 3.7 | M-profile for 05 NOV 89 (over land) | 25 |
| Figure 4.1 | IREPS prediction for 02 NOV 89 (Case 1, 150 MHz) | 32 |
| Figure 4.2 | RPO prediction for 02 NOV 89 (Case 1, 150 MHz) | 32 |
| Figure 4.3 | IREPS prediction for 02 NOV 89 (Case 1, 350 MHz) | 34 |
| Figure 4.4 | RPO prediction for 02 NOV 89 (Case 1, 350 MHz) | 34 |
| Figure 4.5 | IREPS prediction for 02 NOV 89 (Case 1, 3 GHz) | 36 |
| Figure 4.6 | RPO prediction for 02 NOV 89 (Case 1, 3 GHz) | 36 |

| | | |
|--------------------|---|----|
| Figure 4.7 | IREPS prediction for 03 NOV 89 (Case 2, 150 MHz) | 38 |
| Figure 4.8 | RPO prediction for 03 NOV 89 (Case 2, 150 MHz) | 38 |
| Figure 4.9 | IREPS prediction for 03 NOV 89 (Case 2, 350 MHz) | 40 |
| Figure 4.10 | RPO prediction for 03 NOV 89 (Case 2, 350 MHz) | 40 |
| Figure 4.11 | IREPS prediction for 03 NOV 89 (Case 2, 3 GHz) | 42 |
| Figure 4.12 | RPO prediction for 03 NOV 89 (Case 2, 3 GHz) | 42 |
| Figure 4.13 | IREPS prediction for 05 NOV 89 (Case 3, 150 MHz) | 44 |
| Figure 4.14 | RPO prediction for 05 NOV 89 (Case 3, 150 MHz) | 44 |
| Figure 4.15 | IREPS prediction for 05 NOV 89 (Case 3, 350 MHz) | 46 |
| Figure 4.16 | RPO prediction for 05 NOV 89 (Case 3, 350 MHz) | 46 |
| Figure 4.17 | IREPS prediction for 05 NOV 89 (Case 3, 3 GHz) | 47 |
| Figure 4.18 | RPO prediction for 05 NOV 89 (Case 3, 3 GHz) | 47 |
| Figure 5.1 | Ducting across a coastal transition | 52 |

| | | |
|--------------------|---|----|
| Figure 5.2 | RPO inhomogeneous prediction for 02 NOV 89 (Case 1, 150 MHz) | 54 |
| Figure 5.3 | RPO homogeneous prediction for 02 NOV 89 (Case 1, 150 MHz) | 54 |
| Figure 5.4 | RPO inhomogeneous prediction for 02 NOV 89 (Case 1, 350 MHz) | 55 |
| Figure 5.5 | RPO homogeneous prediction for 02 NOV 89 (Case 1, 350 MHz) | 55 |
| Figure 5.6 | RPO inhomogeneous prediction for 02 NOV 89 (Case 1, 3 GHz) | 57 |
| Figure 5.7 | RPO homogeneous prediction for 02 NOV 89 (Case 1, 3 GHz) | 57 |
| Figure 5.8 | RPO inhomogeneous prediction for 03 NOV 89 (Case 2, 150 MHz) | 59 |
| Figure 5.9 | RPO homogeneous prediction for 03 NOV 89 (Case 2, 150 MHz) | 59 |
| Figure 5.10 | RPO inhomogeneous prediction for 03 NOV 89 (Case 2, 350 MHz) | 60 |
| Figure 5.11 | RPO homogeneous prediction for 03 NOV 89 (Case 2, 350 MHz) | 60 |
| Figure 5.12 | RPO inhomogeneous prediction for 03 NOV 89 (Case 2, 3 GHz) | 62 |
| Figure 5.13 | RPO homogeneous prediction for 03 NOV 89 (Case 2, 3 GHz) | 62 |
| Figure 5.14 | Shore to sea prediction for 02 NOV 89 (Case 1, 3 GHz) | 64 |

Figure 5.15 Shore to sea prediction for 03 NOV 89

(Case 2, 3 GHz) 64

I. INTRODUCTION

Control of the electromagnetic (EM) spectrum is essential in today's high technology battle environment. Mastery of the electromagnetic spectrum will ensure continued use of systems that rely on VHF, UHF, SHF, and microwave emissions. To utilize these systems to their fullest capability, it is imperative to understand and exploit any atmospheric effects. Atmospheric anomalies in the troposphere are known to affect VHF, UHF, SHF, and microwave propagation. These anomalies can extend or reduce the effectiveness of electronic emitting systems by bending the propagated waves.

The computer program presently used by the Fleet to predict EM propagation in the atmosphere is the Integrated Refractive Effects Prediction System (IREPS), developed at the Naval Ocean Systems Center (NOSC). With this software, atmospheric effects on electromagnetic propagation can be predicted and exploited. For example, any extended ranges can be predicted and used to advantage. One limitation of IREPS is that it assumes a horizontally homogeneous atmosphere. IREPS predictions are based on empirical formulas and waveguide approximations. A new prediction system under development at NOSC is the Radio Physics Optics Program (RPO) which uses a different predictive technique. Whereas IREPS

relies only on optical ray tracing techniques, RPO also employs parabolic equations which are more theoretically correct and thus provide more accurate EM predictions. However, RPO is calculation intensive and requires more computing time and improved hardware compared to IREPS. This thesis will examine these two programs and compare their signal strength predictions for a coastal environment.

The atmosphere is usually not homogeneous; rather, it is constantly changing both vertically and horizontally. In a coastal environment, propagation anomalies are common due to land-sea differences. For example, surface ducts over the ocean often do not extend onshore. This thesis will examine data from two different sites, one over land and one offshore, to determine how the inhomogeneous coastal atmosphere affects ducting.

IREPS often provides an adequate prediction of duct formation over the offshore ocean, but its assumption of horizontal homogeneity can produce inaccurate results in a coastal environment. RPO is capable of predicting propagation paths for a horizontally inhomogeneous atmosphere. This thesis thus addresses the potential gain of replacing IREPS with RPO for predicting EM propagation near the coast.

Chapter II is background information on atmospheric refractivity and the prediction methods to be compared. In Chapter III, a tactical scenario is developed to illustrate the conditions for which the programs would be used. This

scenario will be evaluated for three different atmospheric environments and for three different frequency bands. In Chapter IV, the scenario is analyzed under identical horizontally homogeneous conditions using both IREPS and RPO to compare the physics of the two models. In Chapter V, the scenario is then analyzed by RPO for horizontally inhomogeneous conditions to evaluate the importance of coastal effects and the errors incurred by assuming horizontal homogeneity. Chapter VI contains the conclusions of the analysis.

II. ATMOSPHERIC REFRACTIVITY

A. GENERAL

The effects of the atmosphere on radio and RADAR propagation have long been of interest to the communications professional. In particular, anomalies caused by inhomogeneities of the refractive index have been observed for decades. In the RADAR spectrum, there have been cases where VHF radio transmissions reached extraordinary distances of over 2000 miles; in 1944, VHF RADAR in Bombay, India was able to map the Persian Gulf coast of Arabia, in detail, from over 1700 miles away. [Ref. 1:p. 12]

Normal, non-anomalous propagation is often based upon the concept of the *standard atmosphere*. A standard atmosphere assumes temperature decreases at a rate of 6.5 degrees centigrade per kilometer of altitude, beginning from a standard sea level temperature of 15 degrees centigrade and pressure of 1013.2 millibars (mb). The concept of the standard atmosphere serves as a starting point for analyzing electromagnetic propagation. [Ref. 2:p. 2-2]

The actual atmosphere, however, often differs from the standard atmosphere. Meteorological phenomena can create conditions which cause electromagnetic waves to be refracted much more than in a standard atmosphere. These conditions

include sharp vertical changes in temperature, sharp vertical changes in humidity, or both. Such temperature and humidity changes are often strongest in the lowest 1000 meters of the atmosphere, and cause many of the significant effects on signal propagation experienced in the VHF, UHF, and RADAR portions of the spectrum. These refractive effects include greatly extended or diminished ranges, transmission fading, duct trapping and leakage, and RADAR/communication holes.

B. ELECTROMAGNETIC SPECTRUM

Electromagnetic waves are refracted, or bent, as they propagate through the atmosphere. Strong refraction can produce anomalous EM propagation. While refraction occurs at all frequencies, it is particularly important at frequencies from 30 MHz to 30 GHz, which includes the VHF, UHF, and RADAR bands. Because the majority of RADARs and communication links utilize this portion of the spectrum, it is vital to understand the effects of refraction and the measurement and prediction methods used. In order to control the electromagnetic spectrum, it is essential that the medium in which waves propagate be understood and correctly modelled.

C. REFRACTIVITY

The term *refractive effects* refers to the property of the lower atmosphere which refracts, or bends, an electromagnetic wave as it passes through the medium. Refraction is caused by

changes in the *index of refraction* of the propagation medium. The most dramatic effect on many naval electromagnetic systems stems from the ducting effect caused by refraction in the troposphere.

The index of refraction, n , is defined as the ratio between the velocity of a wave in free space, c , and the velocity of a wave in a particular medium, v .

$$(1) \quad n = c/v$$

In the earth's atmosphere, the index of refraction varies between 1.000250 and 1.000400. For convenience and ease of calculations, the concept of refractivity, N , has been developed. Refractivity and refraction are related by the following:

$$(2) \quad N = (n-1) \cdot 10^6$$

Refractivity can be calculated directly from measurements of atmospheric pressure, temperature, and humidity.

$$(3) \quad N = 77.6 \cdot (P/T) - 5.6 \cdot (e/T) + 3.73 \cdot 10^5 \cdot (e/T^2)$$

P: Atmospheric pressure in millibars

T: Atmospheric temperature in Kelvin

e: Partial pressure of water vapor in millibars

Another way of representing atmospheric refractive conditions is by the *modified refractivity*, M , which is useful for determining regions of ducting. Modified refractivity and refractivity are linearly related:

$$(4) \quad M = N + 0.157 * h$$

h : Altitude in meters

By plotting modified refractivity against altitude, it can be determined graphically where regions of trapping layers and ducts have formed. Normally, M would increase with increasing altitude; this is a positive dM/dz . A region of negative dM/dz indicates a trapping layer is present. A duct exists below the trapping layer; the boundaries of the duct are explained in the following section. [Ref. 3:pp. 5-7]

D. TRAPPING AND DUCTING

The term *trapping* refers to the refraction of an EM wave for which the wave's radius of curvature is less than that of the radius of curvature of the earth. The EM wave is then refracted back toward the surface of the earth; if it is then reflected off the surface, it will again be refracted back to the earth. This produces *ducting*, which is the channelling of radio or RADAR waves. The EM energy is thus confined to a vertical region, instead of spreading normally. The energy decrease is therefore less than would occur under standard

refractive conditions and produces extended ranges. A trapping layer is necessary to form a duct, but the ducting region can extend beyond the trapping layer. [Ref. 3:pp. 10-11]

Electromagnetic propagation range is extended within the duct. "Holes", where the signal strength is weak and may be below the detection threshold, occur above the ducting region for an antenna which is located within or above the duct. Figure 2.1 depicts the "classic" duct as obtained by "classic" ray tracing prediction methods, which predict a large gradient of signal strength at the top of the duct and zero signal

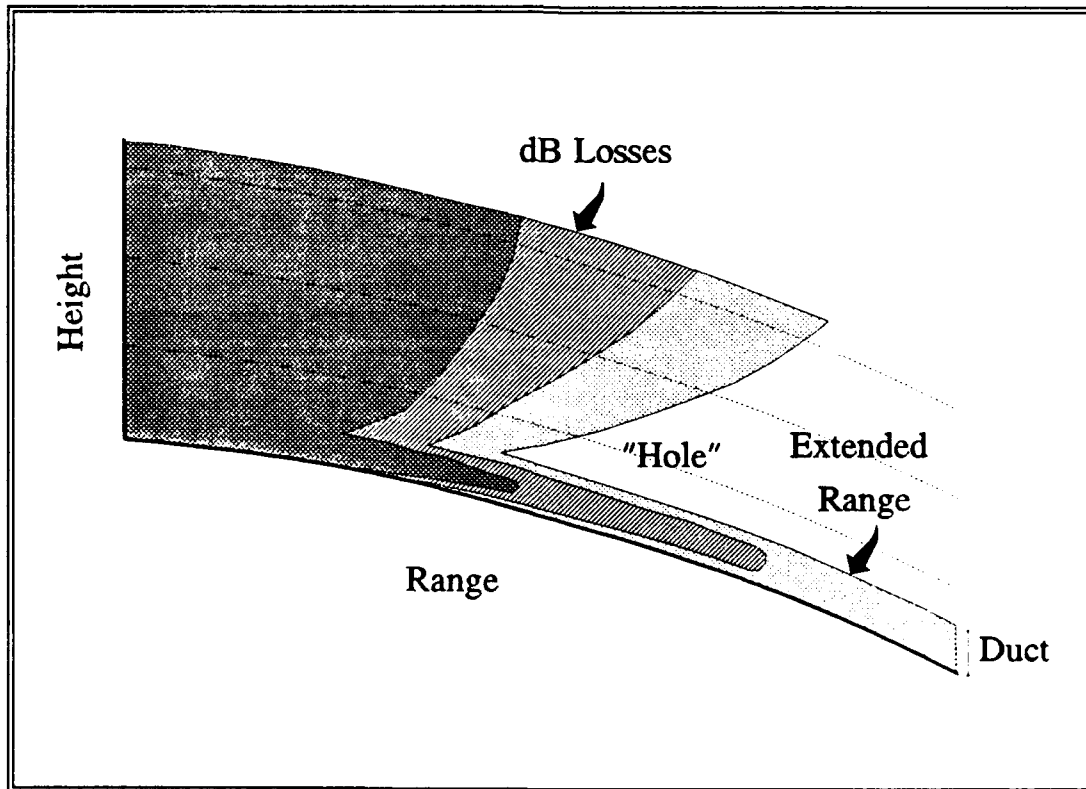


Figure 2.1 Classical ducting

within the hole. In reality, there will be some signal within the hole due to leakage from the duct, allowing for possible signal detection within the hole. This leakage also causes the signal strength within the duct to decrease more rapidly with range. For clarity, Figure 2.1 neglects diffraction, which is the bending of an EM wave along the surface of an obstacle, and interference by surface reflections, which produce lobe-like patterns of signal strength.

The existence of a duct is determined by examining the M-profiles for the atmosphere. This technique is illustrated in Figure 2.2. A trapping layer occurs wherever there is a

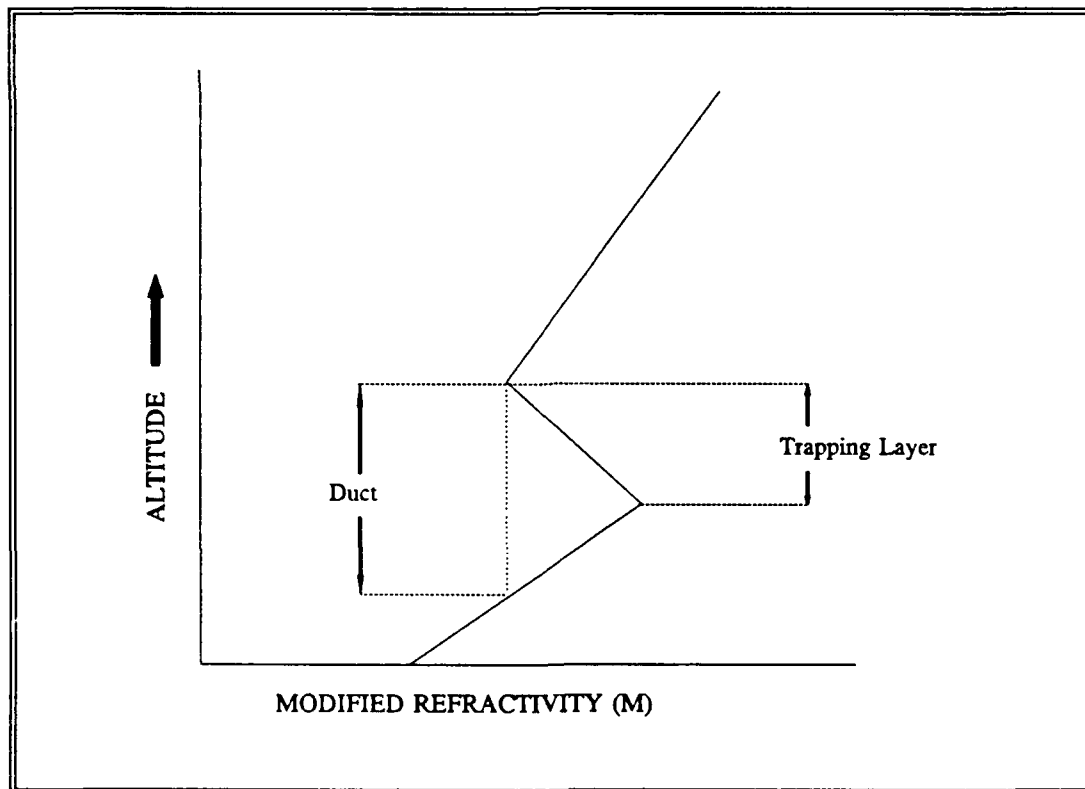


Figure 2.2 Determining duct thickness

negative slope for dM/dz . The duct thickness is then determined by dropping a vertical line from where dM/dz goes from negative to positive (the top of the trapping layer) downward toward the surface. If the vertical line intersects the M-profile prior to reaching the surface, then the duct is elevated. Otherwise, the duct is a surface duct or an evaporation duct.

Ducts can be categorized into three distinct types: evaporation, surface, and elevated ducts. Each type of duct and its associated M-profile is illustrated in Figure 2.3.

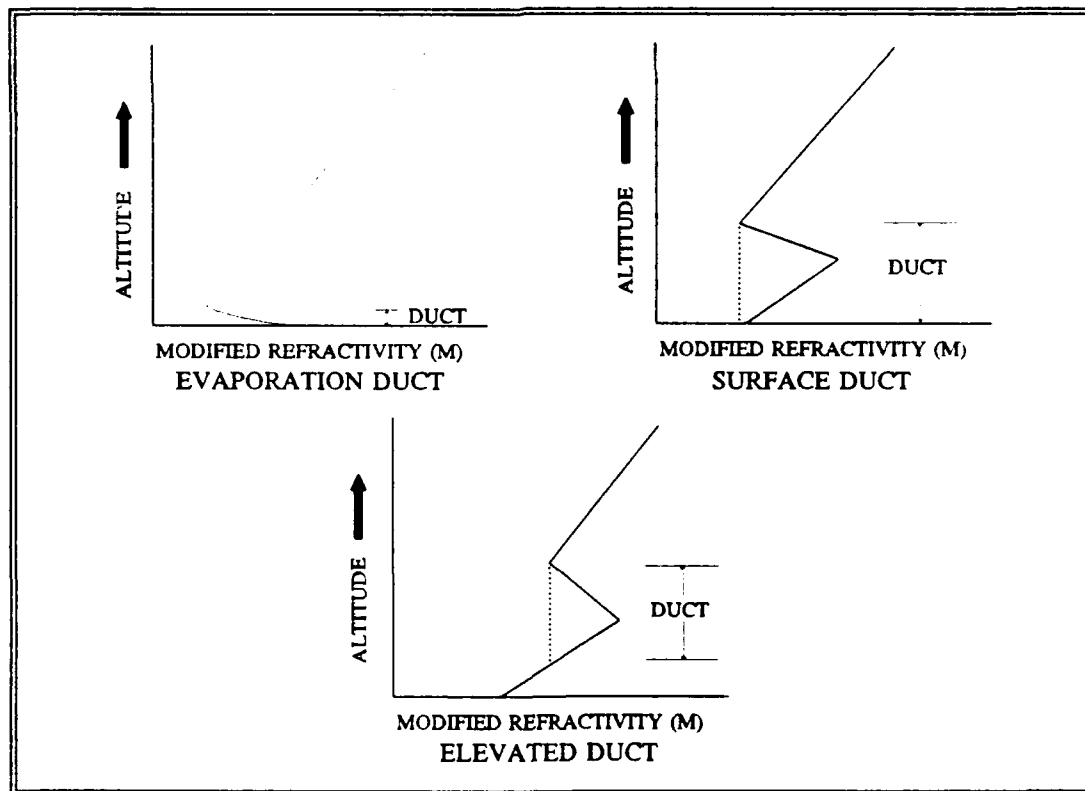


Figure 2.3 Duct types

An evaporation duct generally occurs over water at low altitudes (on the order of less than 30 meters). This type of duct is caused by a rapid vertical decrease in humidity directly over a body of water up to an altitude where the local atmosphere is less humid. [Ref. 2:p. 2-12]

A surface duct is characterized by an M value which, at the top of the trapping layer, is less than the M value at the surface. The surface of the earth acts as the bottom of the duct. A surface duct differs from an evaporation duct in that an evaporation duct is caused strictly by a sharp decrease in the humidity dM/dz gradient whereas temperature dM/dz gradients are also important for surface ducts. Evaporation ducts are formed within a surface layer of atmosphere whereas surface ducts are often caused by temperature inversions aloft; a surface duct is thus usually much deeper than an evaporation duct. Surface based ducts can occur over land as well as over water and generally range between 300m and 1000m in height. [Ref. 2:p. 2-17]

An elevated duct is characterized by an M-profile that contains an inflection point above the surface which is accompanied by an M value which is greater than the M value at the surface. Elevated ducts are often caused by temperature inversions aloft. [Ref. 2:p. 14]

Ducting conditions, however, will not channel all EM frequencies. There is a relationship between the thickness of a duct and the minimum frequency that the duct will channel.

For a given duct thickness, the higher the minimum frequency for a channelled EM wave, the more the wave will be refracted. In order for an EM wave to be trapped, the propagation frequency must be greater than the minimum frequency. This minimum frequency, in Hertz, can be estimated from the following empirical formula:

$$(5) \quad f_{\min} = 3.6 \cdot 10^{11} \cdot d^{-1.5}$$

d: Depth of duct in meters

E. THE COASTAL ENVIRONMENT

With an increasing likelihood of Third World encounters such as the raid on Libya and Operation Desert Storm, the coastal regions have become more important to the Navy's power projection mission. The coastal interface is a relatively abrupt transition between from ocean and land conditions; as such, it has an important impact on ducting conditions and EM propagation. The more accurately this transition can be modelled, the more accurately EM propagation can be predicted.

The boundary layer (BL) results from turbulence created by the earth's surface. There are two major causes of this turbulence: mechanical and thermal. Mechanical turbulence is primarily due to the action of wind flowing over the rough surface media, while thermal turbulence is created by rising bubbles of air created by a heated surface. Because the boundary layer creates dm/dz gradients of temperature and

humidity at its top, it causes the M-profile to change radically within a relatively short vertical distance (less than 20 meters); this often produces a trapping layer at the BL top.

Figure 2.4 shows some of the dynamics of the BL at the coastal interface. The ability of water to mix well and equilibrate its temperature, combined with its higher specific heat, reduces thermal effects on the BL over water. Land, however, is unable to mix for equilibration, so greater heating occurs, which increases the atmospheric turbulence. The diurnal cycle of heating and cooling causes the height of the BL to vary, especially over land.

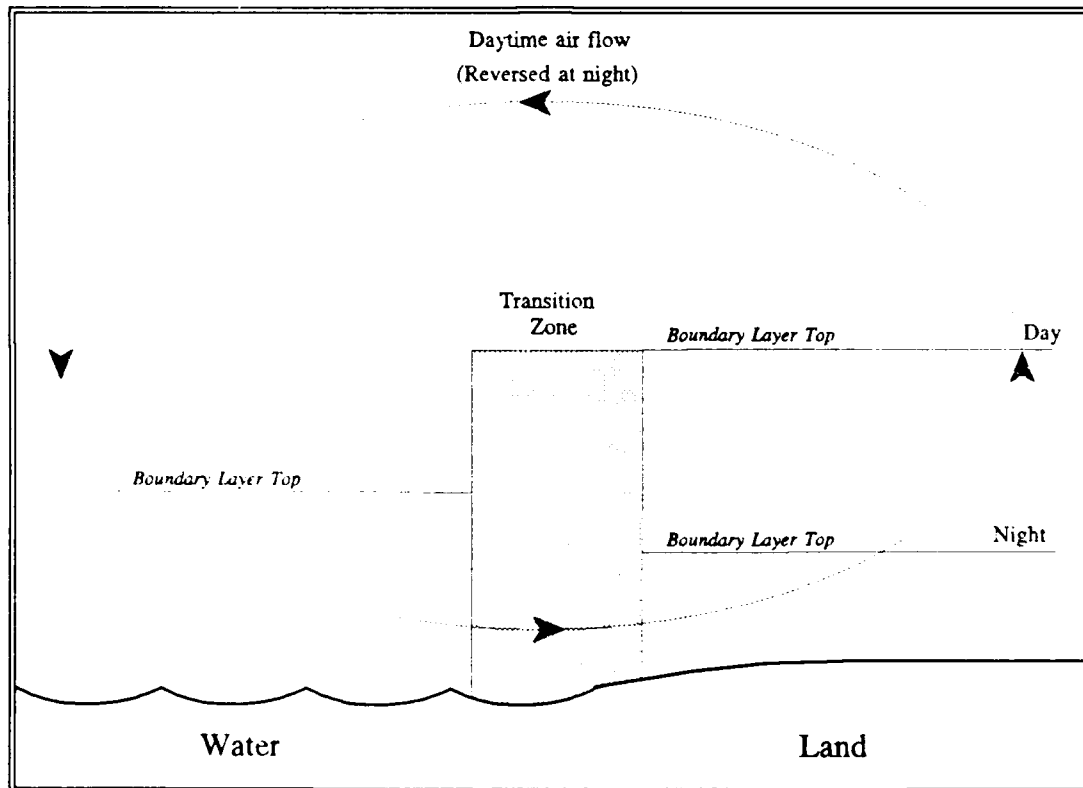


Figure 2.4 The coastal transition

Differential heating over land and water also leads to dynamic effects in the atmosphere, including the diurnal lateral movement of air. The tendency for land to heat and cool faster than the ocean causes sea breezes during the day and land breezes at night, with the cyclic transfer of warm, dry air out to sea and cool, moist air inland during the day; at night, the cycle reverses. This creates a strong interaction between land and water. The daytime subsidence of air over water increases the tendency for ducts to form at sea, while rising air decreases duct formation over land. This cycle reverses at night, but is not as pronounced.

The net result of the process is that the land boundary layer differs markedly from the ocean boundary layer, with the greatest change occurring in the coastal transition zone. There has been a limited amount of work performed on the exact nature of the transition, so for this thesis, all changes in M-profiles are assumed to be linear across the coastal interface.

F. REFRACTIVITY PREDICTION PROGRAMS

1. Integrated Refractive Effects Prediction System

(IREPS)

IREPS was developed at the Naval Ocean Systems Center (NOSC) to provide shipboard environmental data processing and display capability for comprehensive refractive effects assessment of naval surveillance, communications, electronic

warfare, and weapons guidance systems. IREPS has been successfully used under operational conditions aboard most CV/CVNs to assess and exploit refractive effects in tactical situations. [Ref. 2:p. 1-1]

Simple refractive changes in an atmosphere can be modelled by a technique known as geometric ray tracing, which is used by IREPS. Ray tracing traces the path of an EM wave based upon the small angle approximation to Snell's law. [Ref. 3:p. 47] There are limitations to this technique, however. They are:

- The refractive index must not change significantly in a wavelength's distance.
- Spacing between neighboring rays must be small. This avoids confusion when the rays converge, diverge, or cross.
- Constructive or destructive interference is extremely difficult to model.
- Calculated propagation loss of the signal is not exact and must be approximated.

IREPS requires atmospheric data for its calculations. Atmospheric measurements such as temperature, pressure, and relative humidity can be directly entered from which IREPS will calculate an M-profile. If an M-profile has already been calculated, this can be directly accessed. Electronic Warfare data must also be entered. The required data includes frequency, antenna height, antenna pattern, and elevation

angle. IREPS is capable of displaying free space loss ranges or dB losses. Range and elevation units can be either metric or U.S.

IREPS has many features which include:

- Frequency range of 100 MHz to 20 GHz.
- IREPS is based on ray tracing techniques but also includes parameterizations for diffraction.
- Computes signal strength over given height and distance.
- Direct and indirect path interference computed.

IREPS has many limitations, however, which must be understood when assessing its prediction of atmospheric propagation.

- It assumes the surface is an ocean. This prevents use of IREPS over land.
- It assumes that the atmosphere is horizontally homogeneous. This has shown to be a valid assumption approximately 85% of the time over open ocean. However, this is not a valid assumption while operating in a coastal environment.
- Leakage effects, where an EM wave escapes ducting, are neglected.
- Atmospheric absorption is neglected.
- Diffraction effects, which are computed near and beyond the horizon, and tropospheric scatter, important far beyond the horizon, are approximated through empirical equations.

2. Radio Physics Optics Program (RPO)

With the introduction of high speed computers capable of large capacity high speed calculations, new techniques have been developed which better model the actual atmospheric conditions and wave propagation. RPO is one such technique which employs a parabolic wave prediction differential equation. The parabolic equation technique, developed approximately twenty years ago, intrinsically computes the effects of frequency, M-profiles, and spatial distribution of a horizontally inhomogeneous atmosphere upon EM prediction. The parabolic equation is solved via an algorithm called the split-step fast Fourier transform. A major advantage of this technique is that it computes leakage and diffraction effects.

RPO is a hybrid method that uses the complimentary strengths of both the ray tracing model and the parabolic equations. As such, it is able to construct a relatively fast and very accurate composite model. RPO uses the parabolic equations where the EM waves are near horizontal; i.e., inside a duct. Outside of ducting conditions, ray tracing is incorporated. The parabolic equations which RPO uses allow for eleven different horizontal data profiles and can thus more accurately model the true atmosphere and subsequent refractive properties.

RPO is presently under development at NOSC. This thesis tests RPO for its computation abilities, not its user interface. RPO lacks many of the capabilities of IREPS such

as computing M-profiles, displaying a curved earth, entering atmospheric data and antenna parameters directly into the program, and placing an antenna inside an elevated duct. Some of these features would have to be included before RPO could be used by the Fleet.

The advantages of the parabolic equations over ray tracing techniques would be particularly significant when predicting EM propagation in elevated ducts. IREPS, a ray tracing program designed to model surface and evaporation ducts, uses an approximation method to model a duct beyond the optical region; its technique of "template matching" using a height-gain curve is not valid for elevated ducts because of multi-mode propagation. The parabolic equations do not require the multi-mode approximation and thus more accurately model an elevated duct. [Ref. 4:p. 10] However, the ability of the parabolic equations to model elevated ducts has not been fully exploited by RPO as it is limited to antenna heights of not more than 100 meters.

III. METEOROLOGICAL CONDITIONS AND TACTICAL ENVIRONMENT

A. SCENARIO

One mission of the United States Navy is power projection. This means that firepower must be applied to targets over land. Because of the high technology incorporated into modern warfare, knowledge of propagation conditions is essential for successful application of weaponry.

A realistic scenario has been envisioned involving a carrier battle group stationed off the coast of a hostile nation. A surgical strike has been ordered. The main force of the battle group is stationed far enough out to sea to reduce the threat from land based aircraft and shore batteries. A cruiser is designated as the picket ship and is stationed along the threat axis to provide early warning and would be the first to engage hostile aircraft. It is stationed approximately 180 kilometers from the coast. The designated target is a military airfield located approximately 50 kilometers inland. There is a 20 kilometer transitional area, known as the coastal interface, between land and sea. This scenario is illustrated in Figure 3.1.

An aircraft carrier is capable of obtaining M-profiles by launching radiosondes. This will provide conditions over water in the vicinity of the battle group. These conditions

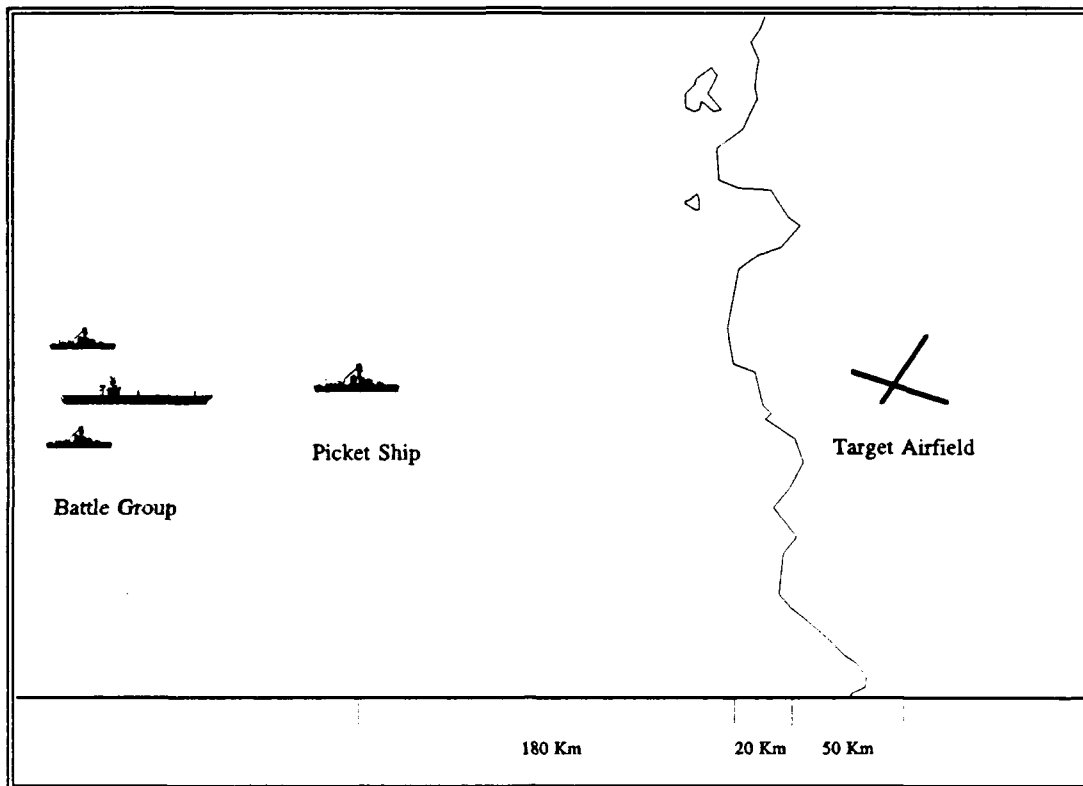


Figure 3.1 Battle group scenario

will be assumed to exist everywhere within the battle group and continue along the propagation path until the coastal interface. This has been shown to be a valid assumption about 85 percent of the time over the open ocean [Ref. 2:p. 3-11].

Obtaining an M-profile over the target area is a difficult task. The developed scenario considers two possibilities:

- The first possibility assumes a homogeneous atmosphere using M-profiles obtained over water. Such might be the assumption if only offshore data were available. Of course, the atmosphere would actually be horizontally inhomogeneous, so assuming a homogeneous atmosphere will introduce error into

the propagation prediction. The horizontally homogeneous analysis is presented in Chapter IV.

- The second possibility for the scenario assumes that an M-profile has been obtained for conditions on shore. The exact method of obtaining such data has not been determined for the analysis. The two M-profiles will provide the data to model the atmosphere as being inhomogeneous. The conditions over land are assumed to be the same everywhere within the vicinity of the sounding. The coastal interface has been assumed to be approximately 20 kilometers, since data was collected 20 kilometers off the Monterey coast. It is within this region that the atmosphere will change the most. The horizontally inhomogeneous analysis is presented in Chapter V.

The models under study do not take into account terrain features. Therefore, the coastal interface has been assumed to be low land and featureless.

B. METEOROLOGICAL CONDITIONS

1. Offshore

Meteorological conditions at sea are based upon data collected on board the research vessel Point Sur, which conducted a research cruise in November 1989. The data has been previously analyzed. [Ref. 5:pp. 20-55] Three case days are selected to be analyzed using both RPO and IREPS. Offshore M-profiles for these days are shown in Figures 3.2-3.4. The data was collected during daytime hours. It is

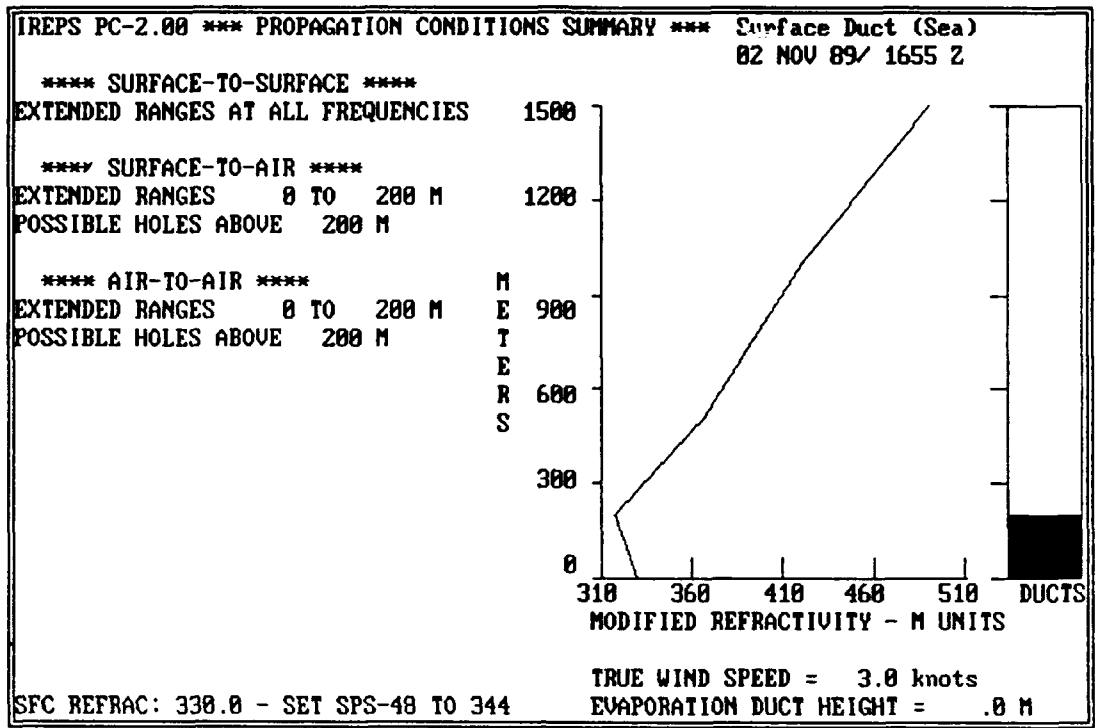


Figure 3.2 M-profile for 02 NOV 89 (offshore)

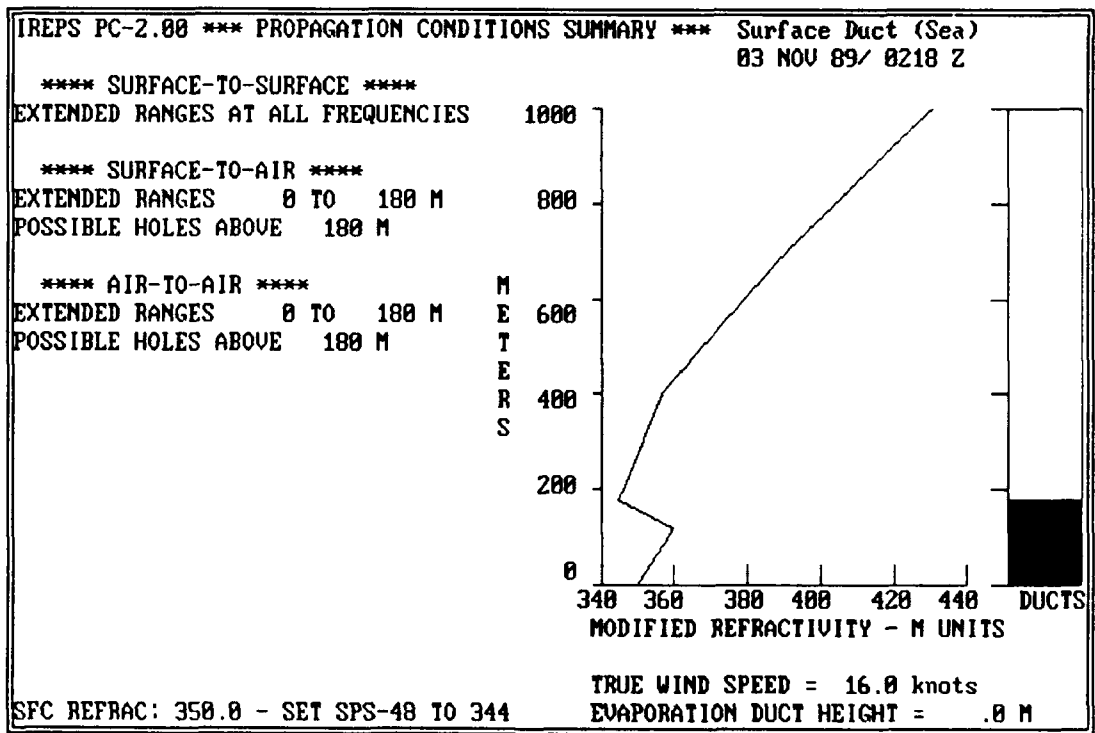


Figure 3.3 M-profile for 03 NOV 89 (offshore)

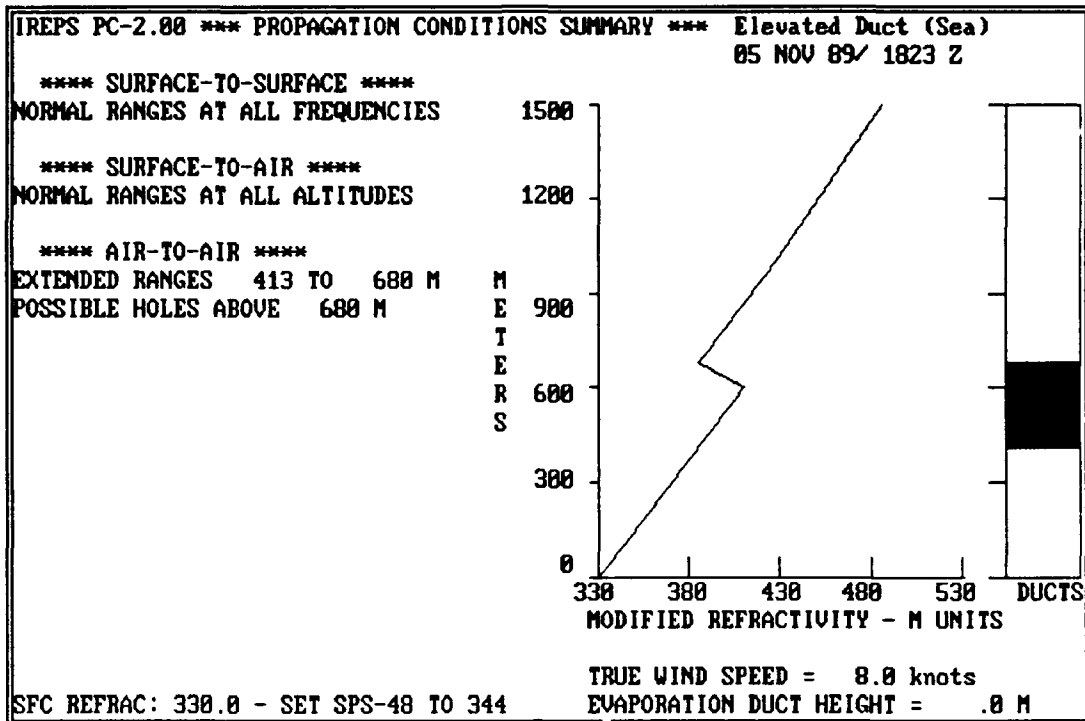


Figure 3.4 M-profile for 05 NOV 89 (offshore)

assumed that the conditions were relatively stable and did not vary significantly over a several hour period.

As can be seen from the M-profiles, ducting conditions exist over water for all three case days. Case 1 is for conditions that existed on 02 November 1989, Case 2 is for conditions that existed on 03 November 1989, and Case 3 is for conditions that existed on 05 November 1989. A surface duct exists for both Case 1 and Case 2. The Case 1 surface duct is composed entirely of a trapping layer. The Case 2 surface duct is created by an elevated trapping layer. For Case 3, an elevated duct exists.

2. Over Land

Meteorological conditions over land for these case days were obtained from soundings made at Vandenberg Air Force Base in November 1989. The raw data was analyzed using IREPS 2.0 and subsequent M-profiles were produced. These profiles are shown in Figures 3.5-3.7.

The time of collection for the Vandenberg data is as closely matched with the research cruise data as possible. There is a maximum five hour difference between soundings. However, as with the cruise data, the soundings were made near the middle of the day. It is assumed that the conditions did not change significantly in that time period. The M-profiles

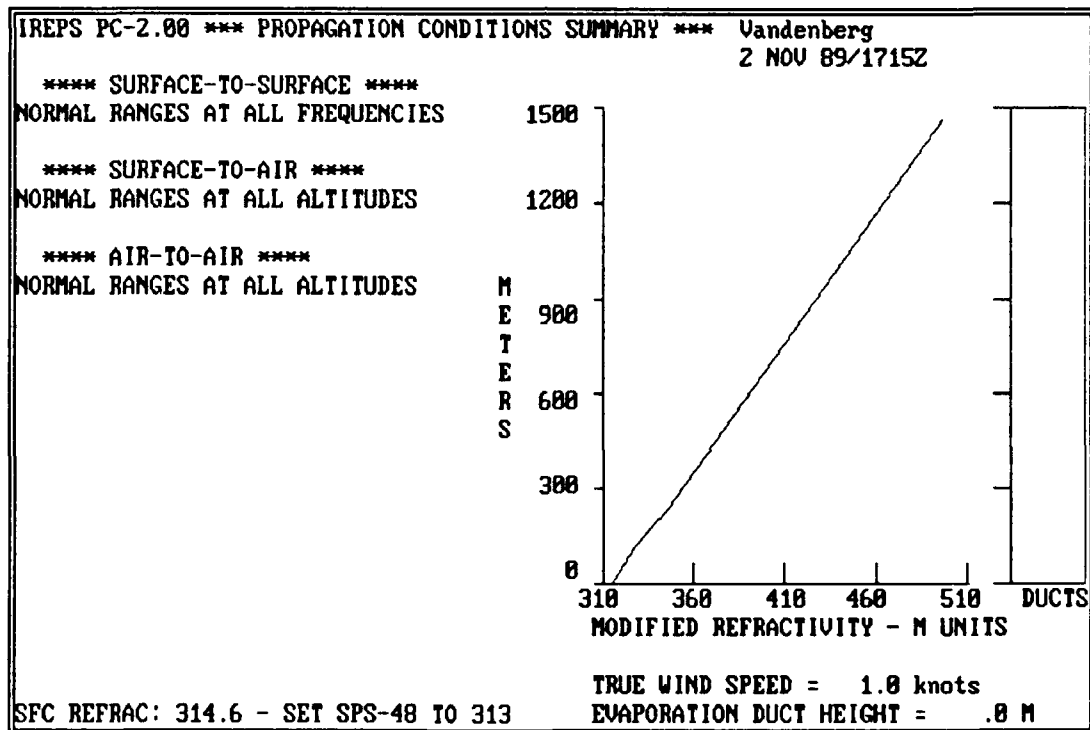


Figure 3.5 M-profile for 02 NOV 89 (over land)

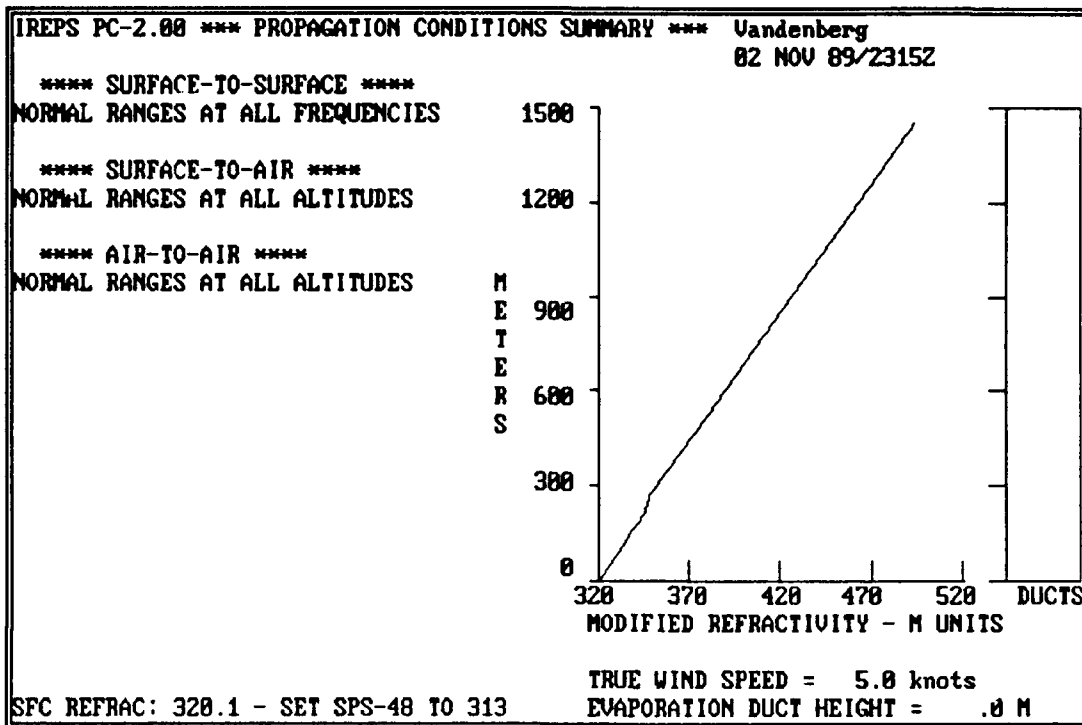


Figure 3.6 M-profile for 03 NOV 89 (over land)

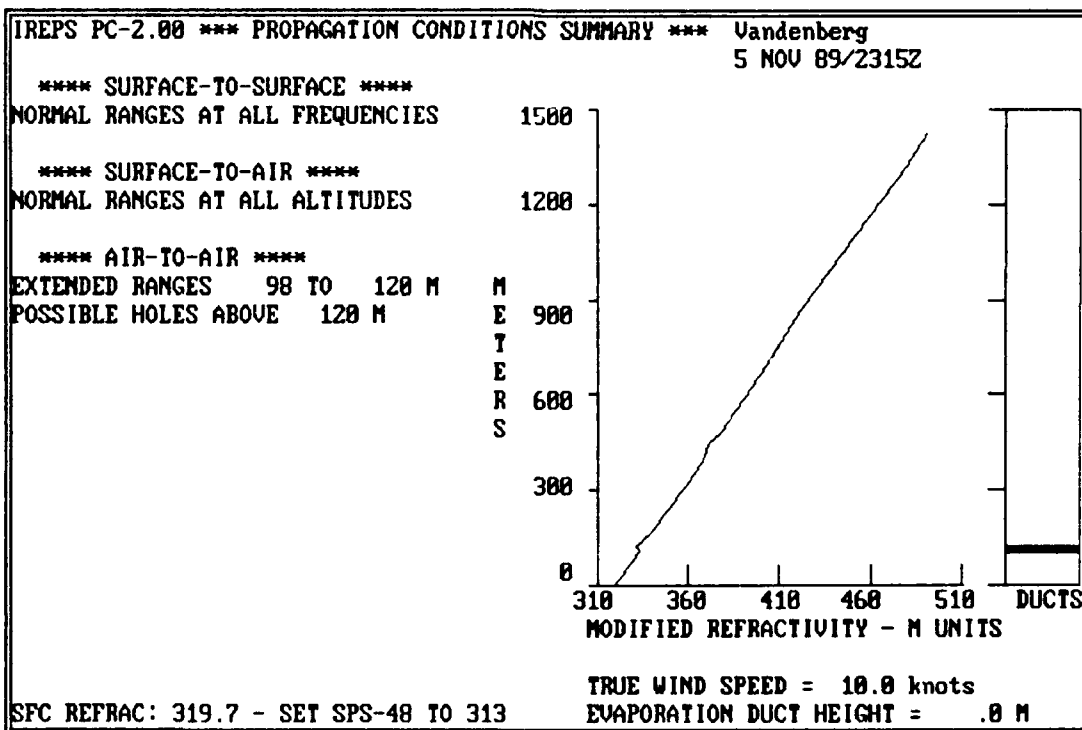


Figure 3.7 M-profile for 05 NOV 89 (over land)

indicate that there are no surface ducts over land for either Case 1 or Case 2 when surface ducts exist offshore. For Case 3, an elevated duct exists over land, thinner and weaker than the one that existed over water.

C. FREQUENCY AND ANTENNA SELECTION

In making the comparison between RPO and IREPS, the scenario calls for three representative "real world" systems, one for each of the VHF, UHF, and RADAR bands.

The Navy uses the VHF spectrum for shipborne and airborne communications. Communications signals are generally non-directional. Therefore, an omni-directional antenna was selected for the analysis. A representative frequency of 150 Mhz is used.

The Navy also uses the UHF spectrum for communications. The requirements for UHF communications are similar to those for VHF. The frequency spectrum is shifted up approximately 200 MHz, so a representative frequency of 350 MHz is used.

The Navy uses many different types of RADAR systems including surface search, air search, and fire control. For illustrative purposes, a shipborne air search RADAR with a representative frequency of 3 GHz (3000 MHz) is selected for comparison. The propagation pattern of an air search RADAR can vary depending upon the specific dimensions of the transmitter. A $\sin x/x$ pattern is selected for the analysis.

The scenario also calls for analysis of a land-based early warning RADAR attempting to locate the battle group. A representative frequency of 3 GHz is selected so that a direct comparison could be made to the ship's tactical picture.

D. SUMMARY

Three propagation prediction methods are employed: IREPS, which must assume a horizontally homogeneous atmosphere, and RPO for both a homogeneous and inhomogeneous atmosphere. For the homogeneous atmosphere, the over water M-profiles are assumed to represent the atmosphere at all locations.

Three meteorological cases are analyzed. Case 1 is for a surface duct over water composed entirely of a trapping layer with no ducting over land. Case 2 is for a surface duct over water composed of an elevated trapping layer with no ducting over land. Case 3 is for an elevated duct over water and a thin weak elevated duct over land based.

Three different frequency bands are tested for each combination. Table 3.1 is a summary of these analysis, which produce a total of 27 (3x3x3) output plots.

The scenario is also analyzed using RPO from the perspective of a shore-based early warning RADAR looking out to sea. Case 1 and Case 2 is used for the analysis, giving two additional analysis.

TABLE 3.1 CASES ANALYZED

| PROPAGATION PREDICTION | METEOROLOGICAL CONDITIONS | FREQUENCY |
|--------------------------------|---|---------------|
| IREPS (Homogeneous Atmosphere) | Surface Duct formed by Surface Trapping Layer (Case 1) | 150 MHz (VHF) |
| RPO (Homogeneous Atmosphere) | Surface Duct formed by Elevated Trapping Layer (Case 2) | 350 MHz (UHF) |
| RPO (Inhomogeneous Atmosphere) | Elevated Duct (Case 3) | 3 GHz (RADAR) |

IV. COMPARISON AND ANALYSIS OF IREPS AND RPO RESULTS FOR A HORIZONTALLY HOMOGENEOUS ATMOSPHERE

A. INTRODUCTION

1. General

This chapter presents the results of the atmospheric propagation prediction models for a horizontally homogeneous atmosphere. IREPS uses ray tracing techniques to model the atmosphere. RPO is a hybrid which uses the parabolic equations as well as ray tracing techniques. The purpose of the analysis is to compare the physics of the two prediction models. Because RPO incorporates the parabolic equations, it directly computes the effects of leakage, interference, and diffraction, which IREPS does not. Thus, it is probable that RPO models the atmosphere more accurately than IREPS, since IREPS often parameterizes or neglects these factors.

2. Output Display

The output of RPO could not be directly compared to IREPS because of software limitations. At present, the RPO display is in a "flat earth" format, whereas the IREPS display is in a "curved earth" form. To allow comparison, RPO predictions are translated into a curved earth format by creating an output file which is displayed by the Engineer's Refractive Effects Predictive System (EREPS). Both IREPS and

EREPS produce color displays of dB thresholds; however, when these are printed in black and white, the cross-hatching schemes used to indicate signal level are not identical from IREPS to EREPS. To make outputs from the two programs comparable, both are programmed to display the same four dB thresholds, with the lowest loss (120 dB) shown at the zero kilometer range marker (the transmitter location). The higher losses are shown at greater distances.

Available path loss, in dB, is selected for the analysis. Loss ranges of 120, 130, 140, and 150 dB are selected, which represent realistic losses for actual systems in use. It is assumed that signal detection can be achieved within these ranges. Beyond 150 dB losses, no detection is assumed.

3. Data Collection

The data for the analysis was collected offshore as described in Chapter III. Because the analysis is for a horizontally homogeneous atmosphere, only one sounding is used for each case.

4. Antenna Lobe Patterns

For 150 MHz and 350 MHz, an omni-directional antenna is selected. For 3 GHz, a $\sin x/x$ antenna is presented for the analysis. To test the effects of antenna pattern differences, omni-directional antenna patterns were run at 3 GHz, but there was no appreciable difference at 3 GHz between an omni-

directional and a $\sin x/x$ antenna. Because RADAR does not normally utilize an omni-directional antenna, the results for an omni-directional antenna are not included in this thesis.

B. CASE 1

1. Environment

The offshore environmental conditions for Case 1, on 2 November 1989 at 1655Z, consisted of a surface duct. As previously shown in Figure 3.1, the surface duct is formed entirely by the trapping layer; i.e., the dM/dz gradient is negative from the surface to the top of the duct.

2. Results for the 150 MHz Analysis

The results of the 150 MHz trials are shown for IREPS (Figure 4.1) and for RPO (Figure 4.2). IREPS predicts marked differences from RPO both qualitatively, in the general shape of the propagation patterns, and quantitatively in signal strength as a function of range. The IREPS program predicts more "classic" ducting effects than does RPO. Both models indicate that the signal will be detected out to the range of the analysis, but signal strength differs greatly between the two predictions. For example, IREPS shows a definite 120 dB duct with greatly extended range (out to 160 km), whereas RPO shows the same signal strength only to 90 km.

A dramatic difference in duct modelling is readily apparent in the comparison for this frequency. IREPS uses a wave guide approximation to model a surface duct beyond the

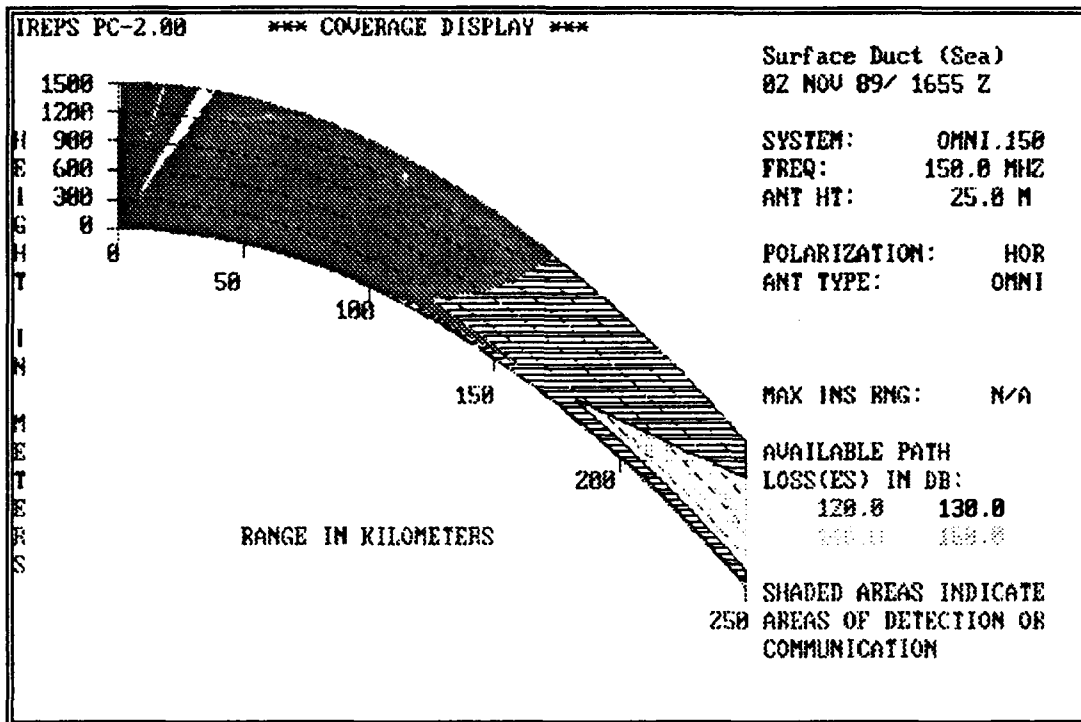


Figure 4.1 IREPS prediction for 02 NOV 89
(Case 1, 150 MHz)

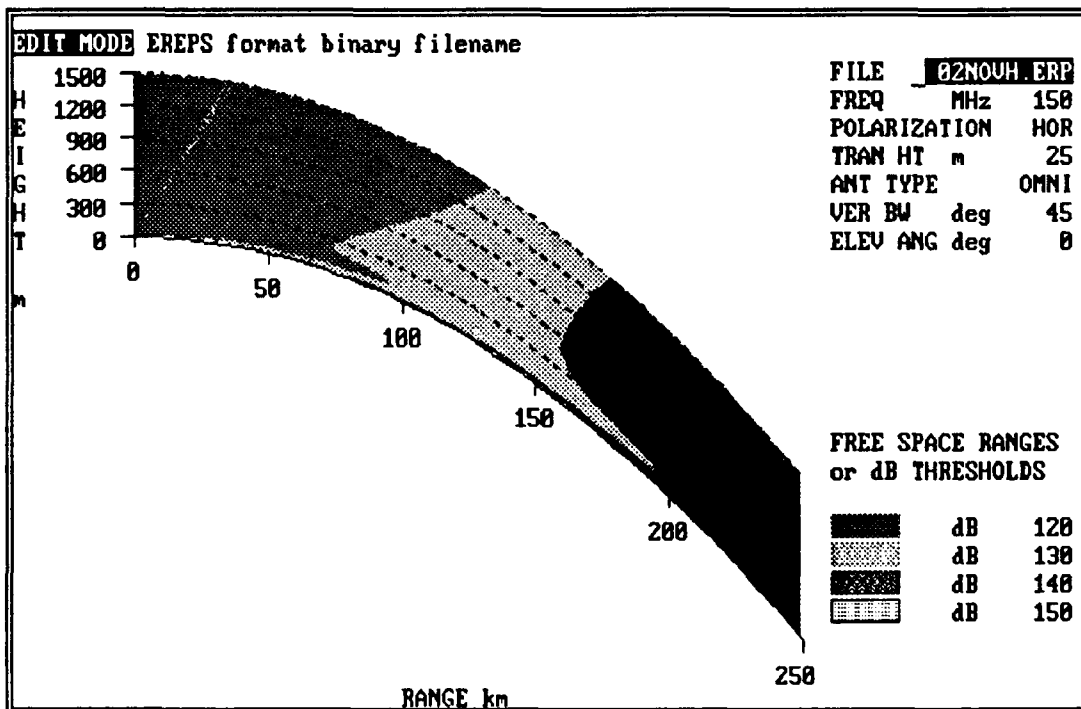


Figure 4.2 RPO prediction for 02 NOV 89 (Case 1, 150 MHz)

radio horizon, whereas RPO calculates the duct strength over the entire range using the parabolic equations. IREPS does predict the general aspects of ducting, illustrated in Figure 4.1: extended range in the duct and a hole above the duct beyond the radio horizon. RPO also predicts ducting and extended range, but the decrease in signal strength above the duct is less dramatic than for IREPS, due to RPO's inclusion of leakage effects, which IREPS neglects.

RPO, in contrast to IREPS, suggests there is a dB loss at the 50, 100, and 150 km range markers near the surface of the earth. This loss may be caused by diffraction (since it is just beyond the radio horizon) and interference. RPO actually computes both of these effects, whereas IREPS only parameterizes diffraction; i.e., it approximates via an empirical formulation, rather than actually calculating the values as does RPO.

3. Results for the 350 MHz Analysis

The results of the 350 MHz trials are shown for IREPS (Figure 4.3) and for RPO (Figure 4.4). Qualitatively, the general pattern of the two models' predictions resemble each other more closely at this higher frequency. Quantitatively, however, the dB path loss ranges for RPO are much shorter than for IREPS, and diffraction effects appear at the surface.

A notable difference between the two models' predictions is the thickness of the duct. For IREPS, the

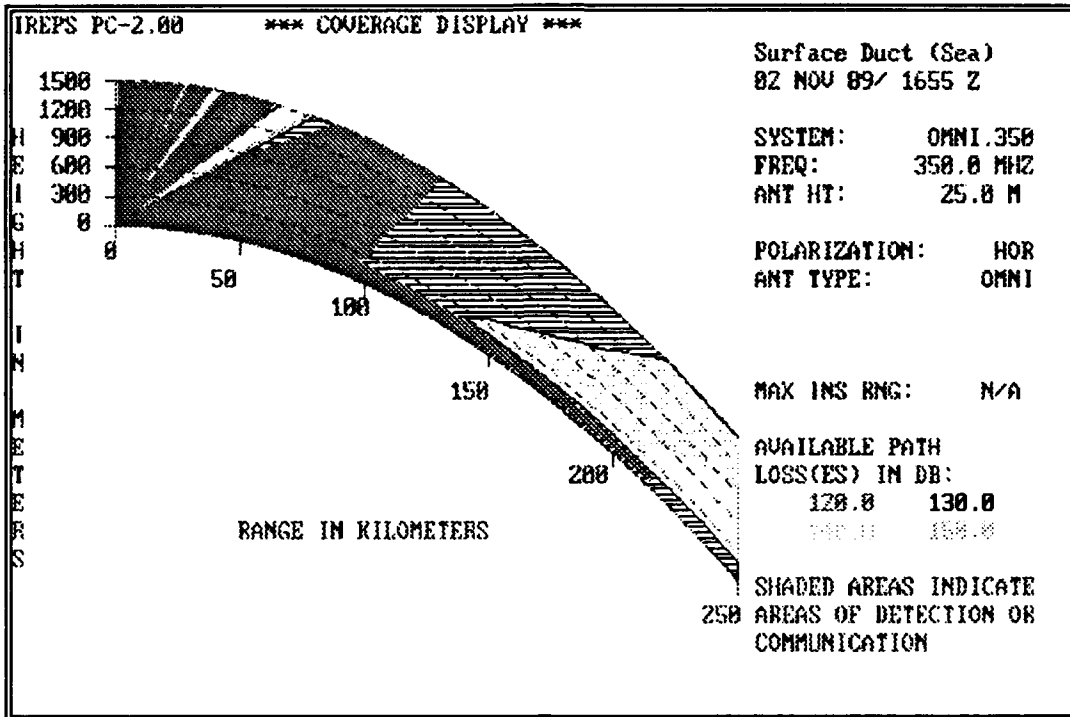


Figure 4.3 IREPS prediction for 02 NOV 89
(Case 1, 350 MHz)

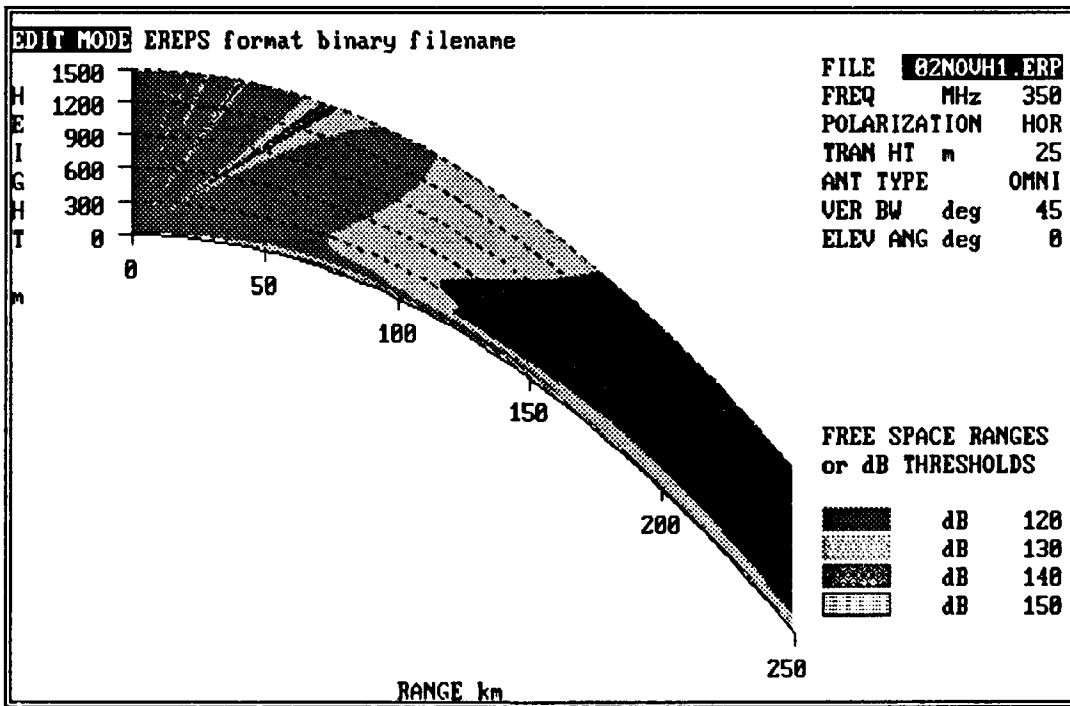


Figure 4.4 RPO prediction for 02 NOV 89 (Case 1, 350 MHz)

frequency effect occurs through the wave guide approximation. RPO, which employs parabolic equations, shows that the height of a given dB contour is not constant with range. The "duct thickness" (as measured by signal strength) increases between 160 and 250 kilometers; i.e., the signal strength decreases with altitude much less rapidly than for IREPS. This is due to the leakage effects neglected by IREPS.

A comparison to the 150 MHz results demonstrates the effect of frequency on ducting. For 150 MHz, RPO does not indicate a classical duct; at the higher frequency, however, a more classic duct does appear. Frequency also has an effect upon IREPS: No holes are apparent for the lower frequency, whereas a hole does appear for the higher frequency.

4. Results for the 3 GHz Analysis

The results of the 3 GHz trials are shown for IREPS (Figure 4.5) and for RPO (Figure 4.6). There are far more interference lobes than at lower frequencies. Although the results are qualitatively similar to each other, RPO provides a more detailed analysis of propagation patterns and expected signal strength as a function of both range and height. For example, IREPS predicts constant signal strength in the extended duct, whereas RPO shows variations throughout.

Both models display classic ducting, with extended range within the duct and a hole beyond the radio horizon. However, RPO predicts a hole within the duct between 210 and

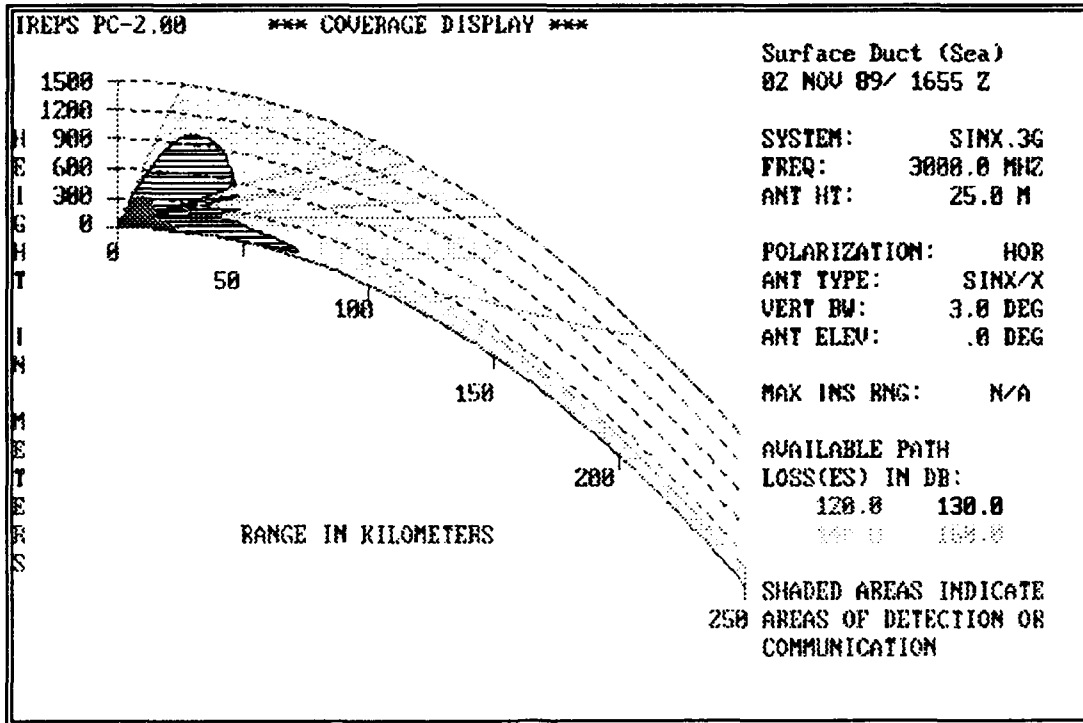


Figure 4.5 IREPS prediction for 02 NOV 89 (Case 1, 3 GHz)

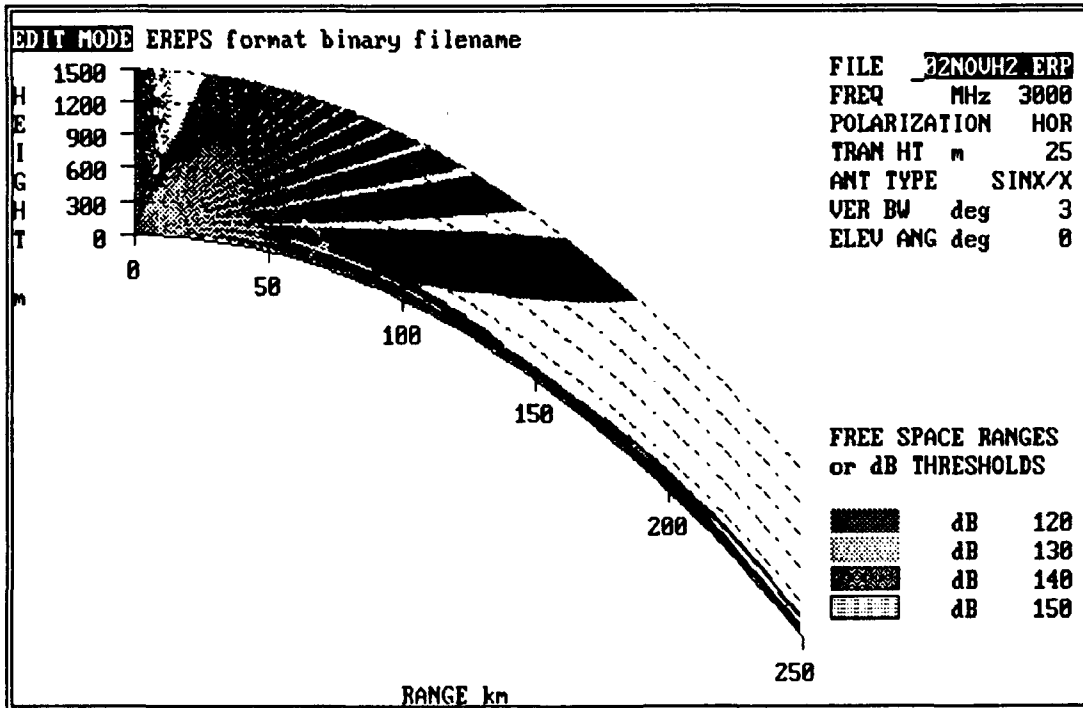


Figure 4.6 RPO prediction for 02 NOV 89 (Case 1, 3 GHz)

250 kilometers. Again, this illustrates the power of RPO, since RPO calculates interference and leakage whereas IREPS only parameterizes interference and neglects leakage effects on signal strength.

C. CASE 2

1. Environment

The offshore environmental conditions for Case 2, on 3 November 1989 at 0218Z, consist of a surface duct which is formed by an elevated trapping layer. As shown in Figure 3.2, the dm/dz gradient has positive slope at low altitude, followed by a reversal of slope to form the trapping layer. Like Case 1, it creates a surface duct, but this form of M-profile yields an entirely different vertical M gradient; therefore, the predictions will differ from Case 1.

2. Results for the 150 MHz Analysis

The results of the 150 MHz trials are shown for IREPS (Figure 4.7) and for RPO (Figure 4.8). These results for an elevated trapping layer show greater differences between IREPS and RPO than did the surface trapping duct of Case 1. While IREPS predictions change only slightly from Case 1 to Case 2, RPO now predicts much enhanced propagation within the duct for Case 2. These EM propagation differences result from the M gradient differences between the two cases.

IREPS predicts the classic shape of a duct, as in Figure 2.1. RPO shows that ducting exists, but the shape is

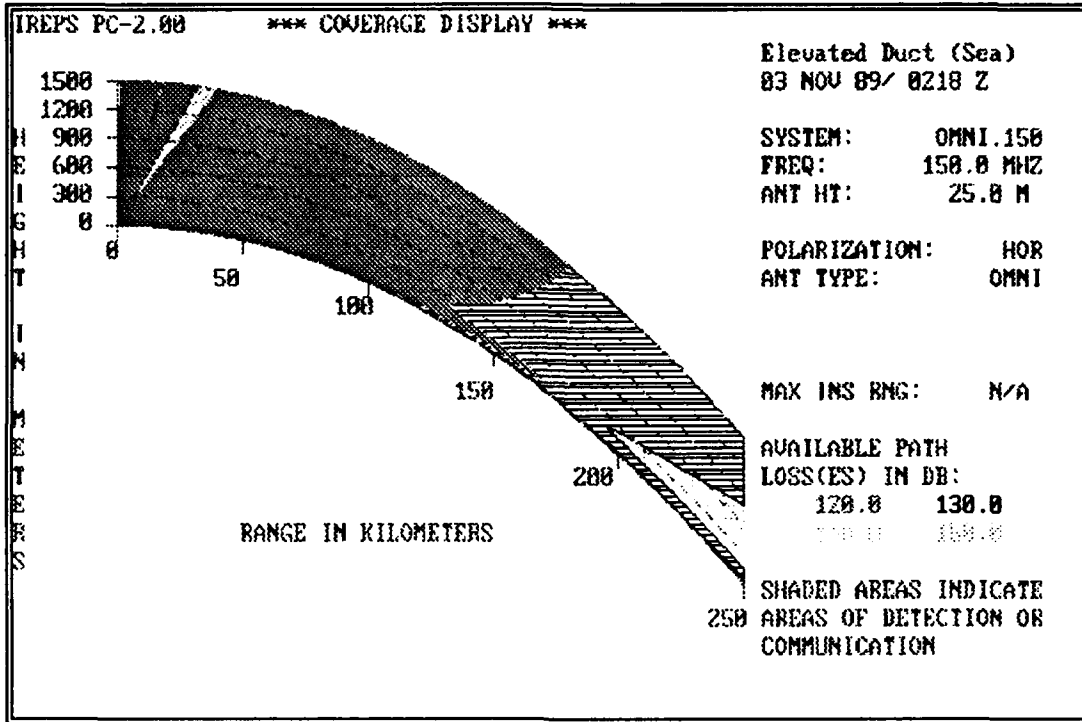


Figure 4.7 IREPS prediction for 03 NOV 89
(Case 2, 150 MHz)

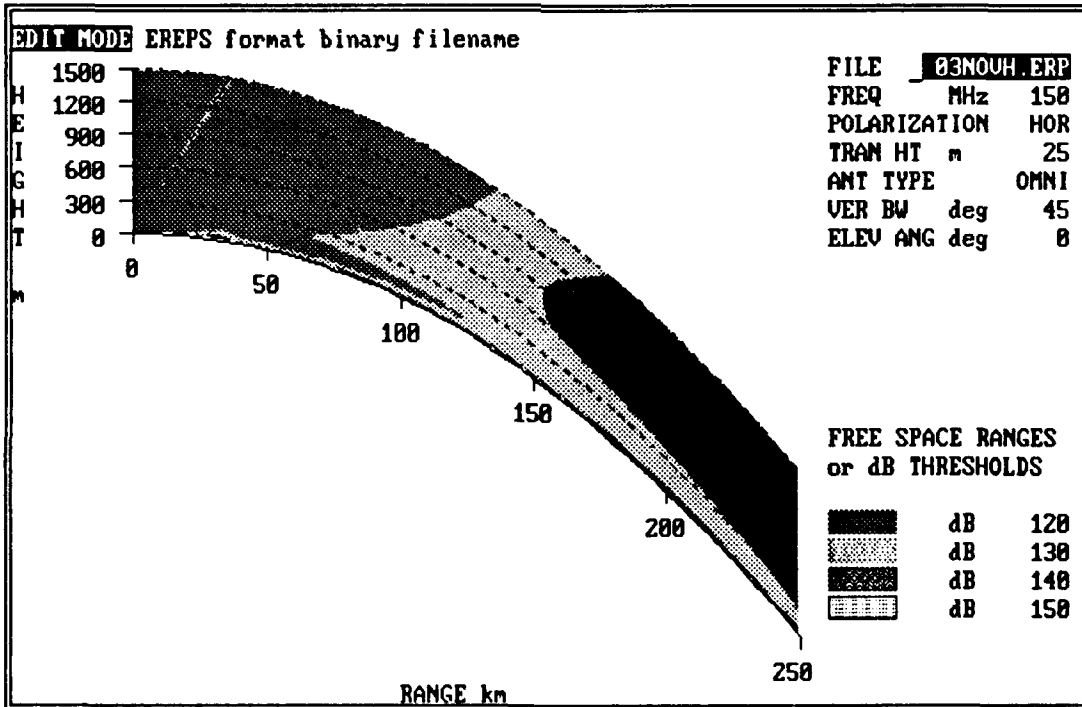


Figure 4.8 RPO prediction for 03 NOV 89 (Case 2, 150 MHz)

not classic. For example, RPO does not show a sharp transition to a duct: at 150 kilometers, the thickness of the 130 dB propagation lobe is 600 meters, and it smoothly narrows to 200 meters at 250 kilometers. IREPS, however, shows a 130 dB duct thickness of 150 meters from 190 km to 250 km. This difference is due to the wave guide approximation of IREPS, whereas RPO uses parabolic equations to calculate signal strength throughout the duct.

3. Results for the 350 MHz Analysis

The results of the 350 MHz trials are shown for IRFPS (Figure 4.9) and for RPO (Figure 4.10). Although similarities between RPO and IREPS are still apparent, RPO produces a more detailed prediction, particularly at shorter ranges. IREPS' predictions are more homogeneous; i.e., a propagation lobe tends to be of uniform signal density, rather than having internal areas of greater or lesser signal strength. This is a result of RPO's use of the parabolic equations instead of ray tracing.

As with Case 1 at this frequency, RPO appears to show diffraction at the surface, because the effect occurs near and beyond the radio horizon. This is particularly noticeable at the 50, 100, and 150 kilometer ranges. IREPS indicates a hole has developed at 220 kilometers, whereas RPO predicts signal detection at all ranges. IREPS also predicts a constant duct thickness starting at approximately 150 kilometers. RPO

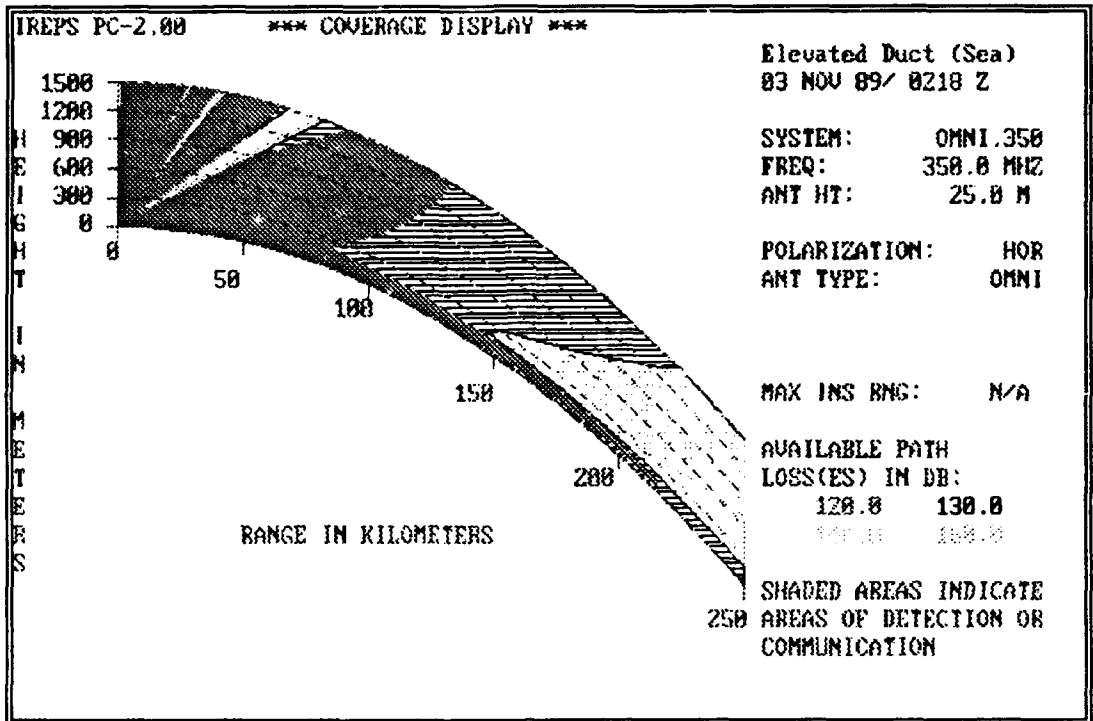


Figure 4.9 IREPS prediction for 03 NOV 89
(Case 2, 350 MHz)

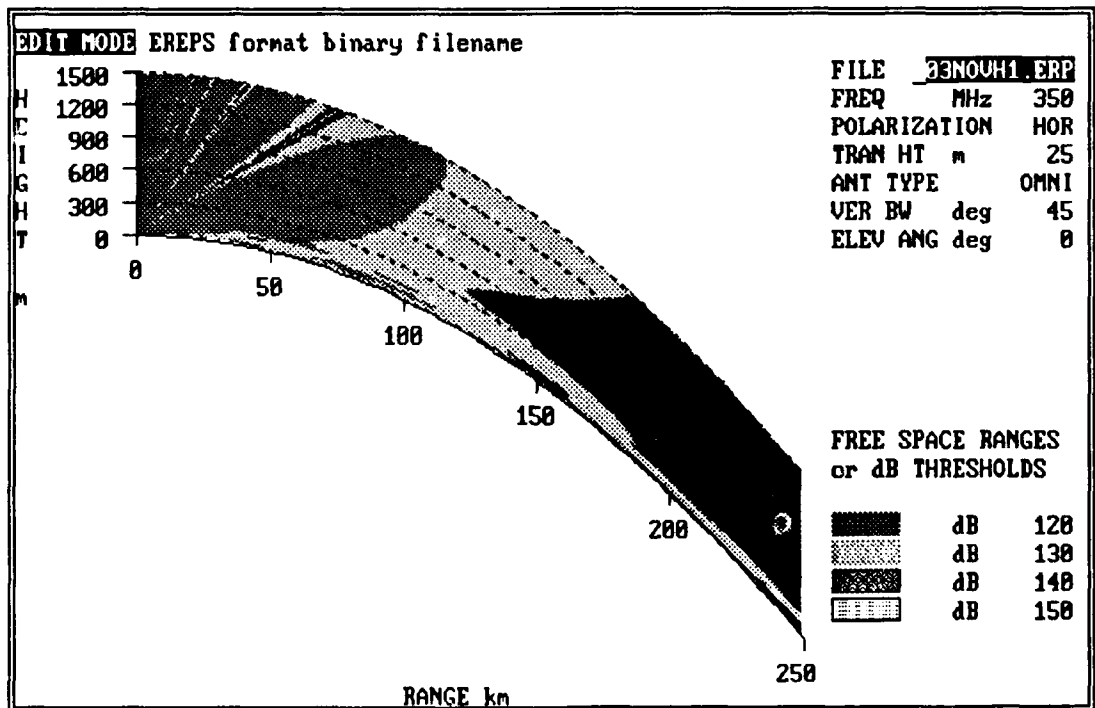


Figure 4.10 RPO prediction for 03 NOV 89 (Case 2, 350 MHz)

predicts the duct thickness changes with range; additionally, at 230 kilometers, the signal strength is reduced at the surface.

4. Results for the 3 GHz Analysis

The results of the 3 GHz trials are shown for IREPS (Figure 4.11) and for RPO (Figure 4.12). At this frequency, the two analyses are qualitatively similar to the results presented in Case 1. Quantitatively, RPO's ability to compute signal strength predicts greater variation within the duct than does IREPS.

5. Interaction Between Duct dM/dz Gradient and Frequency

A comparison between Case 1 and Case 2 predictions illustrates that frequency and duct dM/dz gradient affect the predictions of RPO far more than IREPS. This is first demonstrated for 150 MHz, as seen by comparing Figures 4.1 and 4.7 (IREPS) with Figures 4.2 and 4.8 (RPO). In this comparison, the only change in the environment is from the surface trapping layer of Case 1 to the elevated trapping layer of Case 2 (with a concomitant change in the duct dM/dz gradient). IREPS predicts little difference between the two types of ducts, but RPO does. At 150 MHz, RPO predicts 130 dB duct propagation a minimum of 60 kilometers further for the elevated trapping layer case than for the surface trapping layer case.

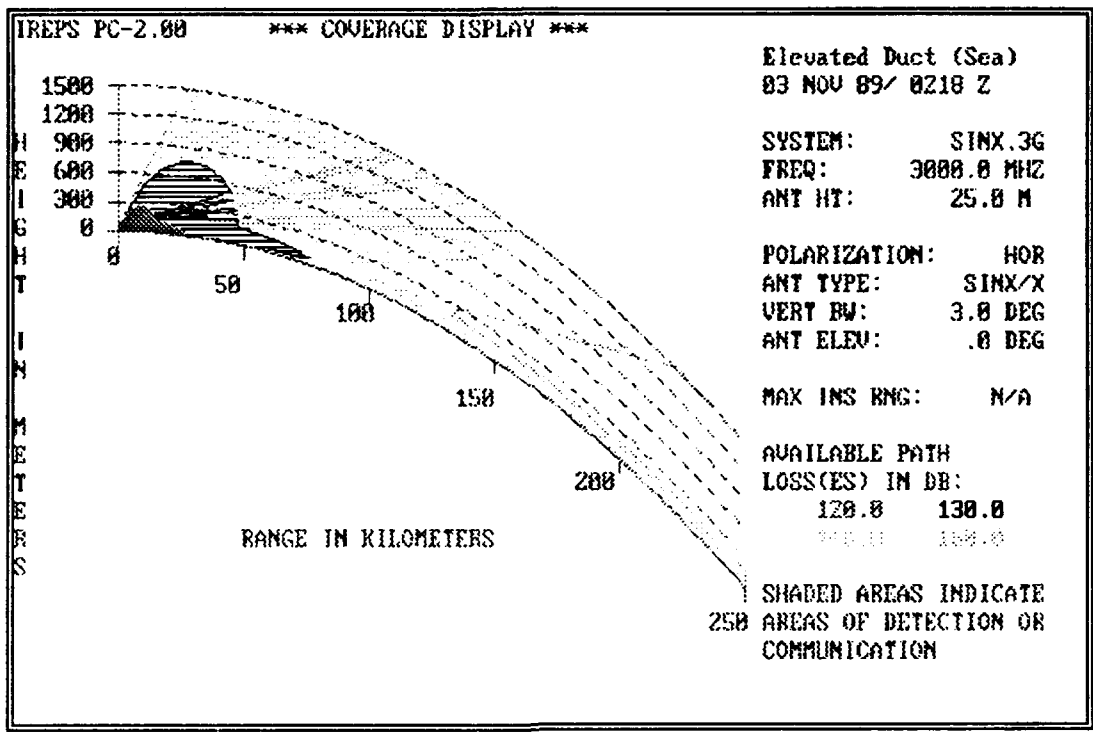


Figure 4.11 IREPS prediction for 03 NOV 89 (Case 2, 3 GHz)

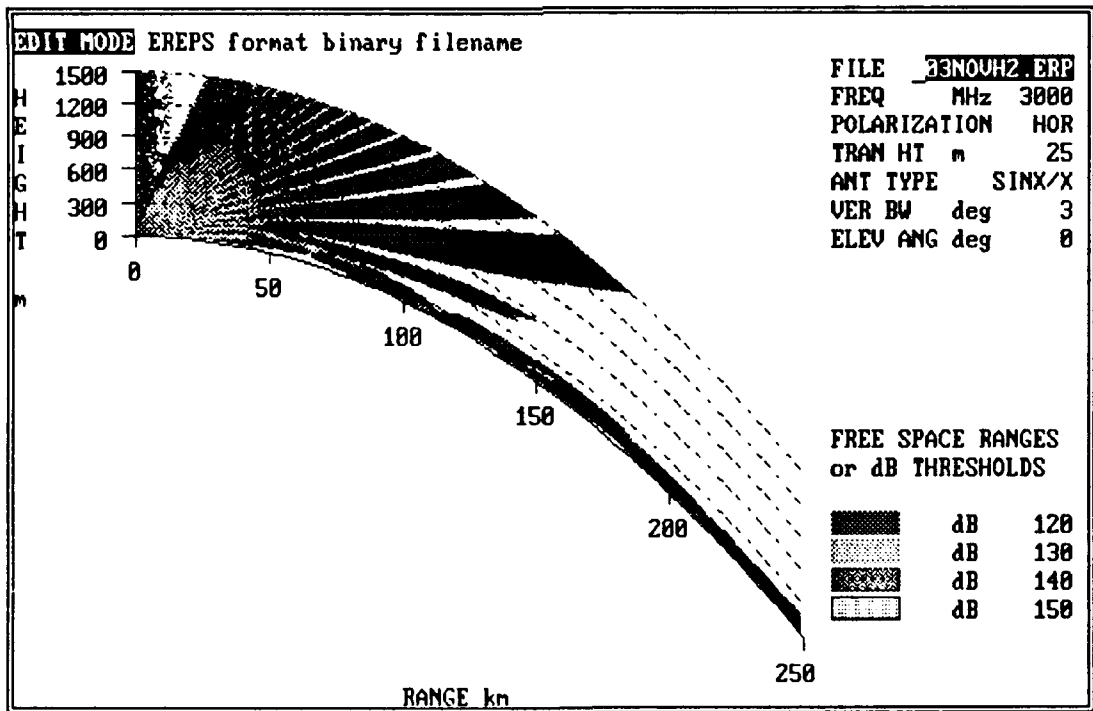


Figure 4.12 RPO prediction for 03 NOV 89 (Case 2, 3 GHz)

At 350 MHz, RPO predicts much greater channelling effect (and a larger hole) for the surface trapping layer than for the elevated trapping layer. This effect is most noticeable for the 130 dB contour, but is also present in the 120 dB contour. This type of interaction cannot be predicted a priori; rather, it must be computed by the parabolic equations.

D. CASE 3

1. Environment

The offshore environmental conditions for Case 3, on 5 November 1989, consist of an elevated duct. This was shown in Figure 3.3. The elevated duct is above the height of the antenna for this case. This analysis is not done for an antenna in the duct, because RPO does not guarantee accurate results for an antenna located above 100 meters; however, this is not an inherent limitation of the parabolic equations.

2. Results for the 150 MHz Analysis

The results of the 150 MHz trials are shown for IREPS (Figure 4.13) and for RPO (Figure 4.14). Because the antenna is below the duct, neither output shows extended ranges of coverage. However, there is a notable difference between the two models' predictions. Whereas IREPS predicts no holes inside propagation lobes, RPO clearly shows that the signal strength is not necessarily constant within lobes. The power of RPO is that it can predict such great detail.

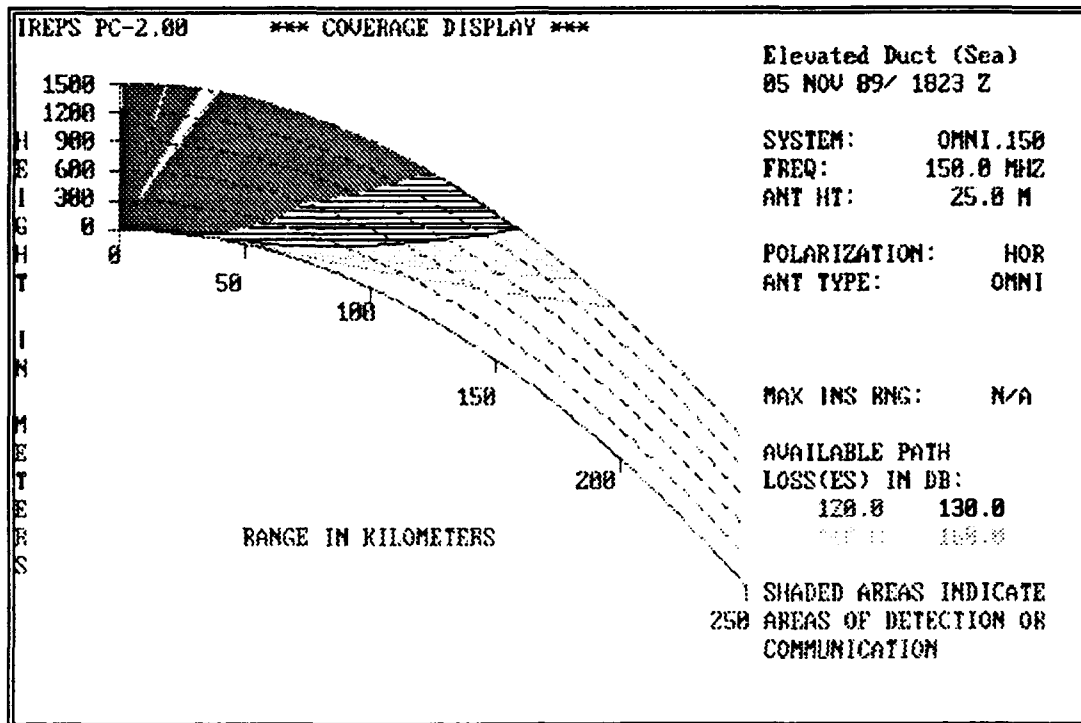


Figure 4.13 IREPS prediction for 05 NOV 89
(Case 3, 150 MHz)

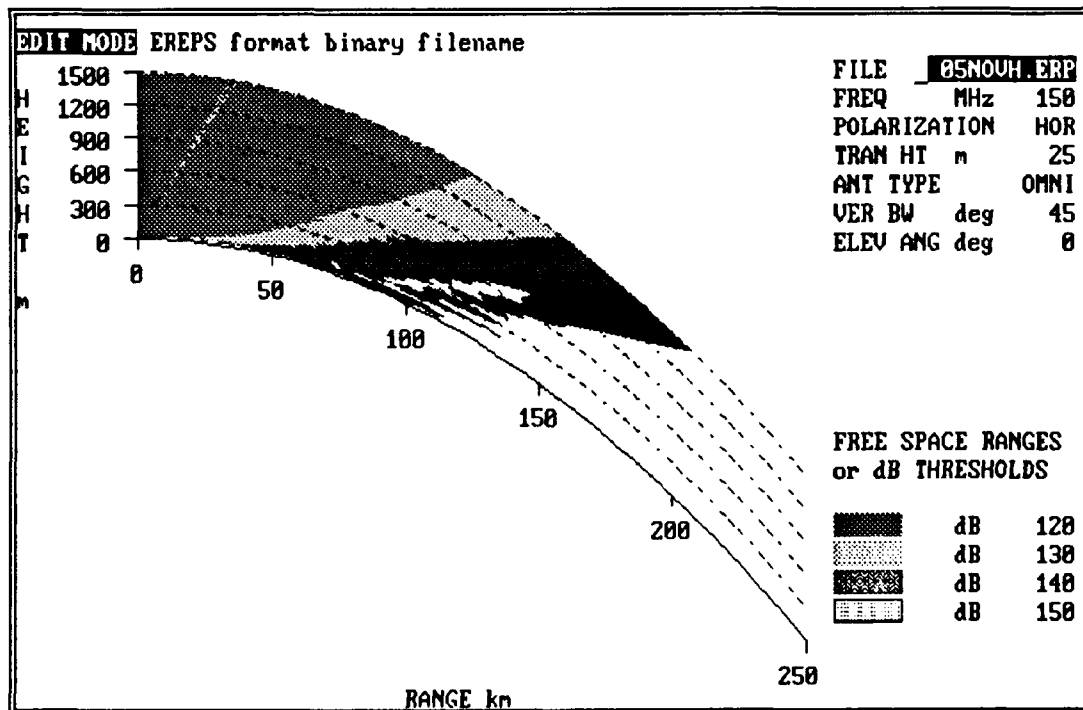


Figure 4.14 RPO prediction for 05 NOV 89 (Case 3, 150 MHz)

3. Results for the 350 Mhz Analysis

The results of the 350 MHz trials are qualitatively similar for IREPS (Figure 4.15) and for RPO (Figure 4.16). There are no major quantitative differences between the two models' predictions. The hole that appeared in the 150 MHz analysis, for RPO, has disappeared at this higher frequency. RPO shows some leakage effects at a range of 100 km at 300 meters, which is the height of the elevated duct. RPO can calculate leakage because it uses the parabolic equations; IREPS completely neglects this effect.

4. Results for the 3 GHz Analysis

The results of the 3 GHz trials are shown for IREPS (Figure 4.17) and for RPO (Figure 4.18). There are no significant differences between IREPS and RPO for this trial. RPO predicts more of the internal structure of the lobes than IREPS. The leakage effect for RPO, which is apparent at lower frequencies, does not appear at 3 GHz.

E. SUMMARY

IREPS uses ray tracing techniques to model the atmosphere, whereas RPO is a hybrid which also incorporates the parabolic equations. As a result, RPO can directly compute the effects of leakage, interference, and diffraction in a duct, whereas IREPS cannot.

Major differences between IREPS and RPO predictions are found for the two surface duct cases where the antenna is in

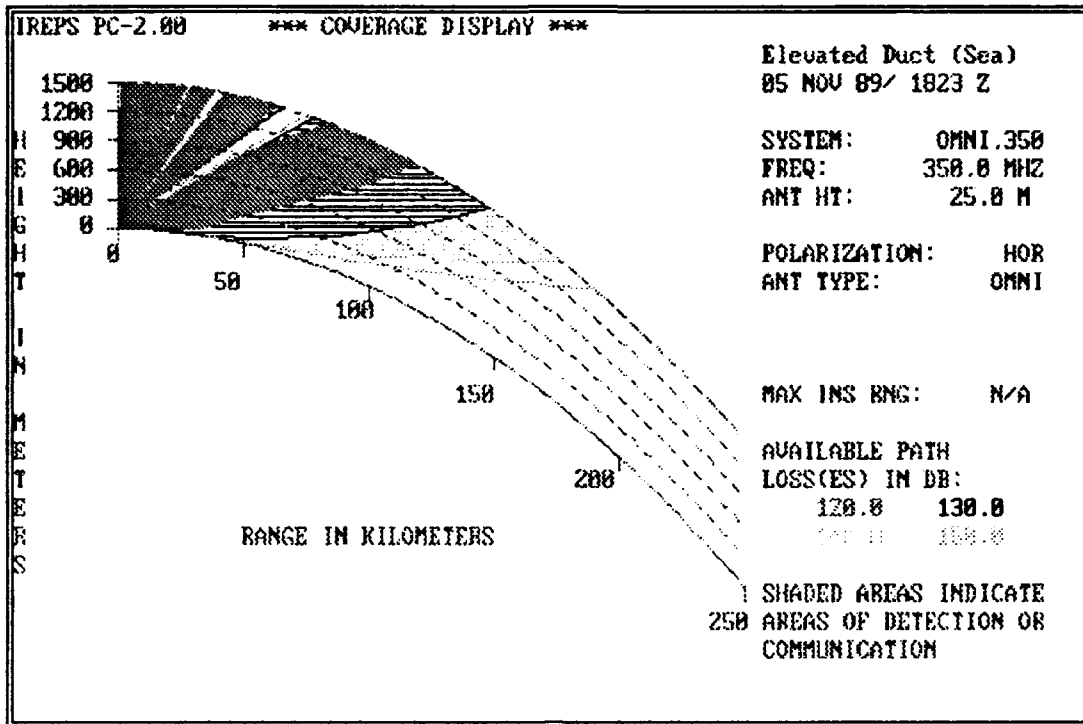


Figure 4.15 IREPS prediction for 05 NOV 89
(Case 3, 350 MHz)

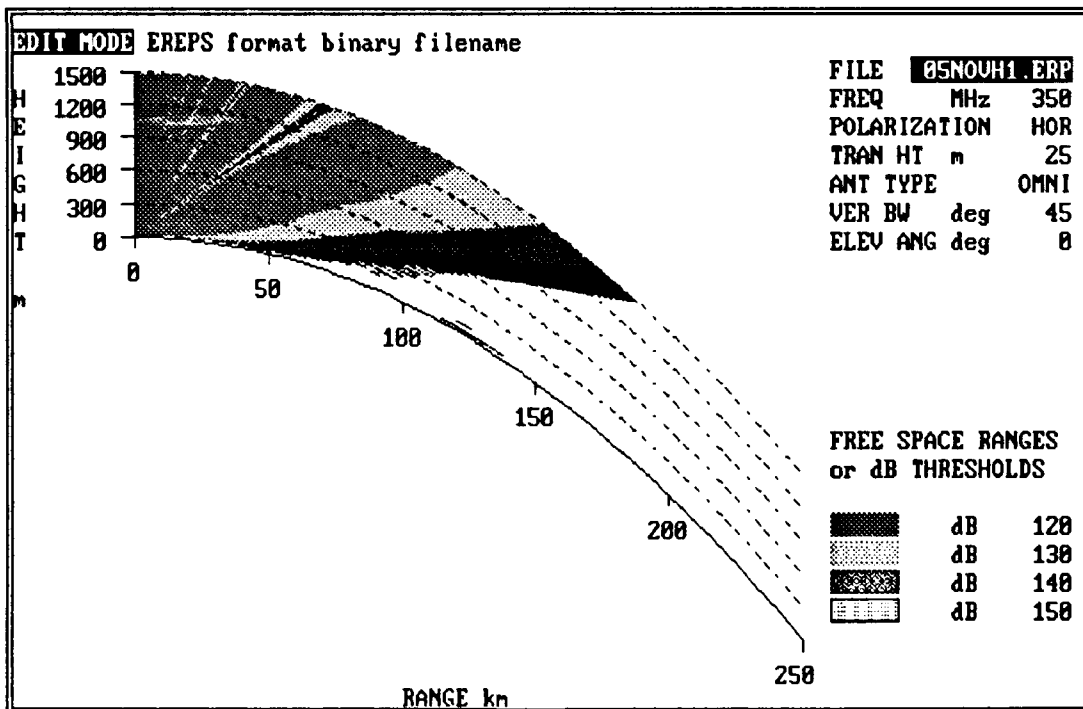


Figure 4.16 RPO prediction for 05 NOV 89 (Case 3, 350 MHz)

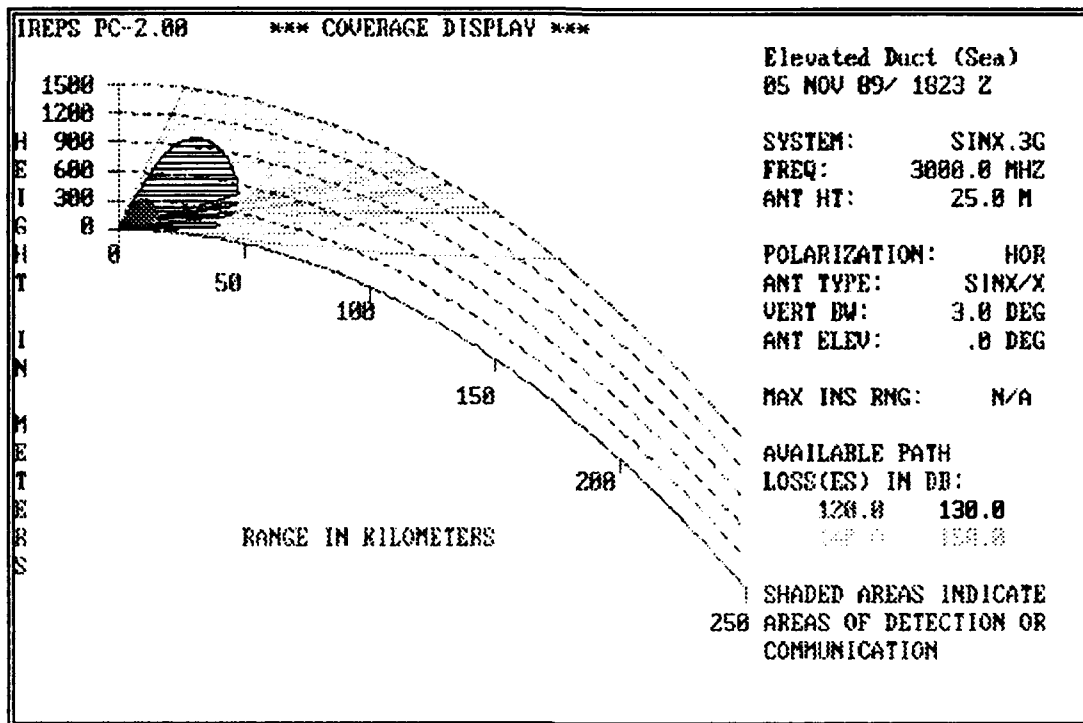


Figure 4.17 IREPS prediction for 05 NOV 89 (Case 3, 3 GHz)

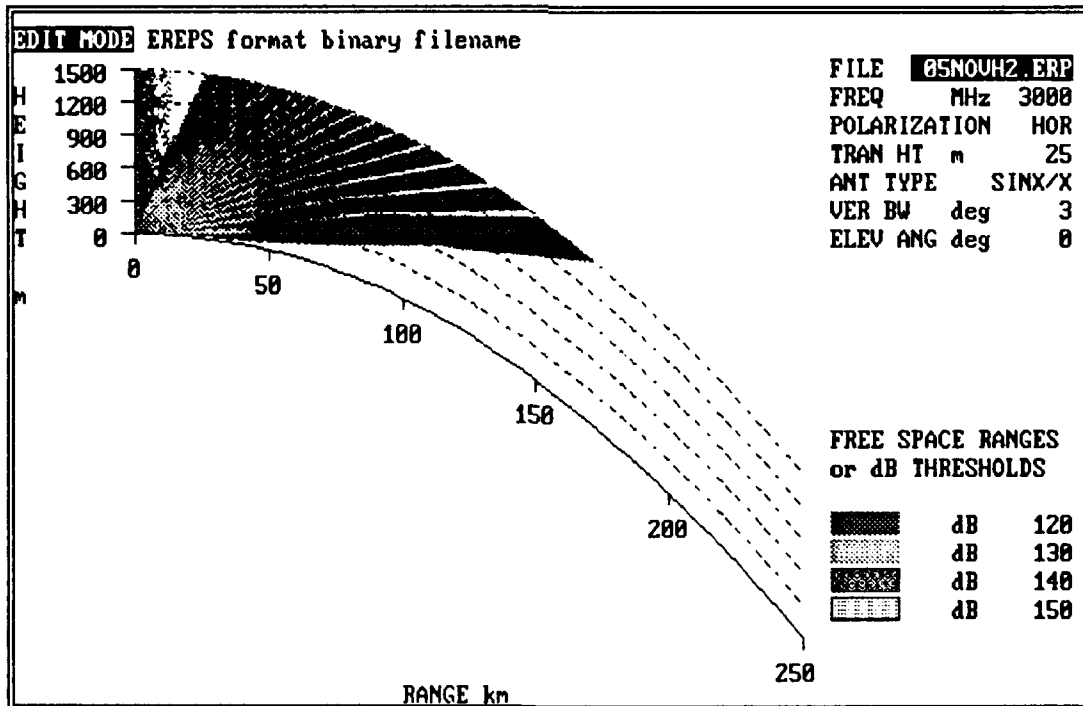


Figure 4.18 RPO prediction for 05 NOV 89 (Case 3, 3 GHz)

the duct, both qualitatively, in the general shape of the propagation patterns, and quantitatively in signal strength as a function of range. Only minor differences are predicted for the elevated duct case, where the antenna is below the duct.

IREPS predicts the "classic" duct effects, such as the artifact of a complete hole above the duct. IREPS can only indicate the general features of ducts, such as extended range and a hole in the coverage, and it always does so in a very idealized fashion. Since IREPS uses a wave guide approximation to model surface ducts beyond the radio horizon, there is little variance in duct thickness as range increases; also, the level of signal in the coverage hole is artificially low with IREPS, because it cannot account for leakage.

RPO directly computes signal strength at all altitudes and ranges, and therefore predicts variations in duct thickness and height. Because RPO calculates leakage, it more accurately predicts signal strength and indicates the finer structure of the propagation pattern. The leakage eliminates the artifact of a complete hole in the coverage above the duct, giving instead a reduced signal strength in the coverage hole. Due to leakage from the duct, there is less signal remaining to be channelled so RPO tends to show shorter propagation ranges in the duct than does IREPS.

RPO often suggests a dB loss near the surface of the earth, which is not predicted by IREPS. This loss is probably caused by diffraction and interference effects. RPO directly

computes both of these effects, whereas IREPS only parameterizes diffraction; i.e., it approximates via an empirical formulation. RPO can thus accurately predict how signal strength will vary within the lobes.

RPO is far more sensitive to changes in duct dM/dz gradient and frequency than is IREPS. IREPS predicts almost no propagation difference between Case 1 and Case 2, which are surface ducts of approximately the same height but formed by very different dM/dz profiles; for RPO, however, the two cases give radically different predictions. With RPO, the predictions for Case 1 and Case 2 also change with frequency: Case 1 causes considerably more ducting effect for the higher frequencies, whereas Case 2 causes the lower frequencies to propagate noticeably farther. IREPS does not predict this frequency effect, which illustrates the weakness of using a parameterized approximation.

The elevated duct is above the height of the antenna for Case 3, so there is minimal coupling of energy into the duct. Significant differences between predictions from the two models occur only at 150 MHz. Predictions could not be obtained for an antenna in the duct, because RPO does not guarantee accurate results with an antenna located above 100 meters.

The significant prediction differences between IREPS and RPO are a consequence of the different physics of the two models. It is probable that RPO models the atmosphere more

accurately than IREPS, since IREPS parameterizes or neglects factors such as leakage, interference, and diffraction.

In a tactical environment, the environmental conditions tested in this chapter would generally result in IREPS overestimating the detection range within the duct, and underestimating it within the coverage hole. In addition, IREPS cannot accurately account for the propagation changes caused by different dm/dz profiles interacting with different frequencies. These differences could lead to use of incorrect or ineffective tactics, and a reduction in mission accomplishment.

V. ANALYSIS OF RPO RESULTS FOR A HORIZONTALLY INHOMOGENEOUS ATMOSPHERE

A. INTRODUCTION

This chapter compares EM predictions in a horizontally inhomogeneous atmosphere with those from a horizontally homogeneous atmosphere. RPO can model either atmospheric condition, whereas IREPS can only model a homogeneous atmosphere. The results of Chapter IV provide the RPO predictions for the horizontally homogeneous atmosphere.

The analysis is done for a change in atmospheric conditions across a coastal transition, as described in Chapter III. Two soundings were obtained; one over land and one offshore. The purpose of this analysis is to show how RPO can be used to model this transition and the errors which can result when horizontal homogeneity is incorrectly assumed.

The assumptions made in Chapter IV concerning dB path loss, signal detection, and antenna lobe patterns remain the same. For ease of comparison, the inhomogeneous atmosphere predictions are accompanied by the homogeneous atmosphere predictions.

B. CASE 1

1. Environment

To perform the RPO analysis in a horizontally inhomogeneous atmosphere, both the sea and land M-profiles are used (Figures 3.2 and 3.5). To simplify the analysis, it is assumed the M-profiles do not change markedly over land or water outside the coastal transition. RPO performs a linear interpolation between M-profiles. The effects of the coastal transition are modelled by entering the M-profiles into RPO as follows: at ranges of 0 and 180 kilometers, the sea profile is used; at ranges of 200 and 250 kilometers, the land profile is used. RPO then maintains a horizontally homogeneous atmosphere between the ship and the coastal transition (0 to 180 kilometers), performs a linear interpolation across the transition (180 to 200 kilometers), and then uses a horizontally homogeneous atmosphere from the edge of the coastal transition to the land-based target of interest at the 250 kilometer range. The effect on ducting is shown in Figure 5.1. The analysis is conducted for the three meteorological cases at the three representative frequencies of 150 MHz, 350 MHz, and 3 GHz.

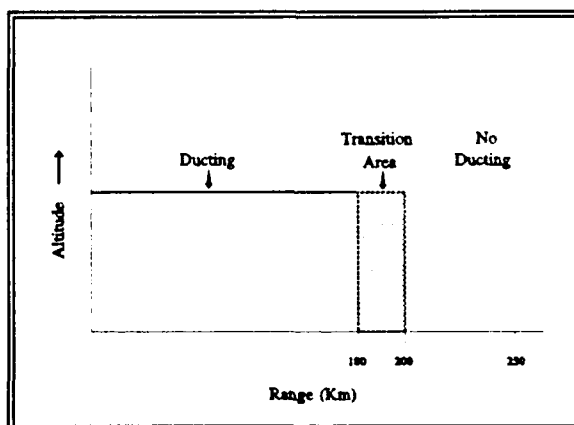


Figure 5.1 Ducting across a coastal transition

2. Results for the 150 MHz Analysis

The 150 MHz predictions are shown in Figures 5.2 and 5.3. The homogeneous and inhomogeneous atmospheric propagation predictions are identical offshore, prior to the coastal transition (i.e., for the first 180 kilometers). This results from forcing RPO to use a horizontally homogeneous atmosphere between these two points. Changes do occur at the coastal transition. Over land, at approximately 210 kilometers, the inhomogeneous prediction shows a region of no signal detection beginning at the surface and rising to an approximate altitude of 100 meters at a range of 250 kilometers. With the duct absent, signals are no longer channelled. Normal spreading of the signal therefore occurs, and signal strength decreases more rapidly with distance. The hole at the surface beyond 220 km is due to the radio horizon, which appears now because the duct ends at 180 km. The signal now decreases normally with distance (as $1/R^2$, where R is distance), instead of the usual duct effect ($1/R$ reduction) inside. The net effect is that of a weak transmitter located at the 180 km marker, with no duct present.

3. Results for the 350 MHz Analysis

The 350 MHz predictions are shown in Figures 5.4 and 5.5. Again, both predictions are identical for the first 180 kilometers, before the coastal transition. At the coastal transition, where the duct disappears, the region of greatest

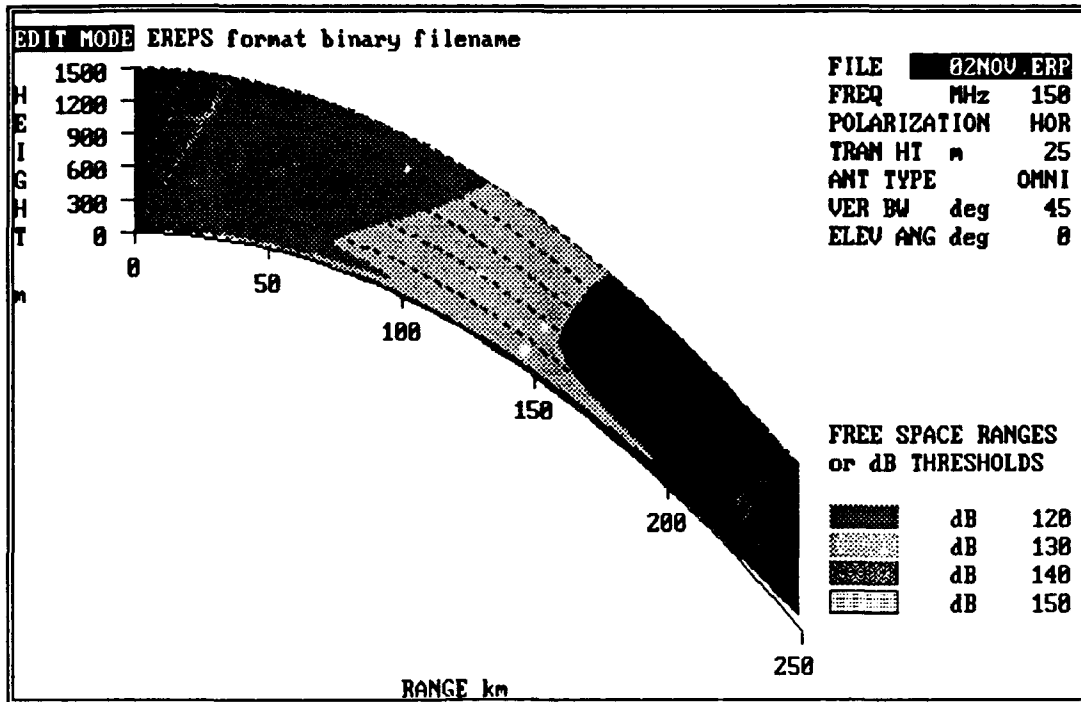


Figure 5.2 RPO inhomogeneous prediction for 02 NOV 89 (Case 1, 150 MHz)

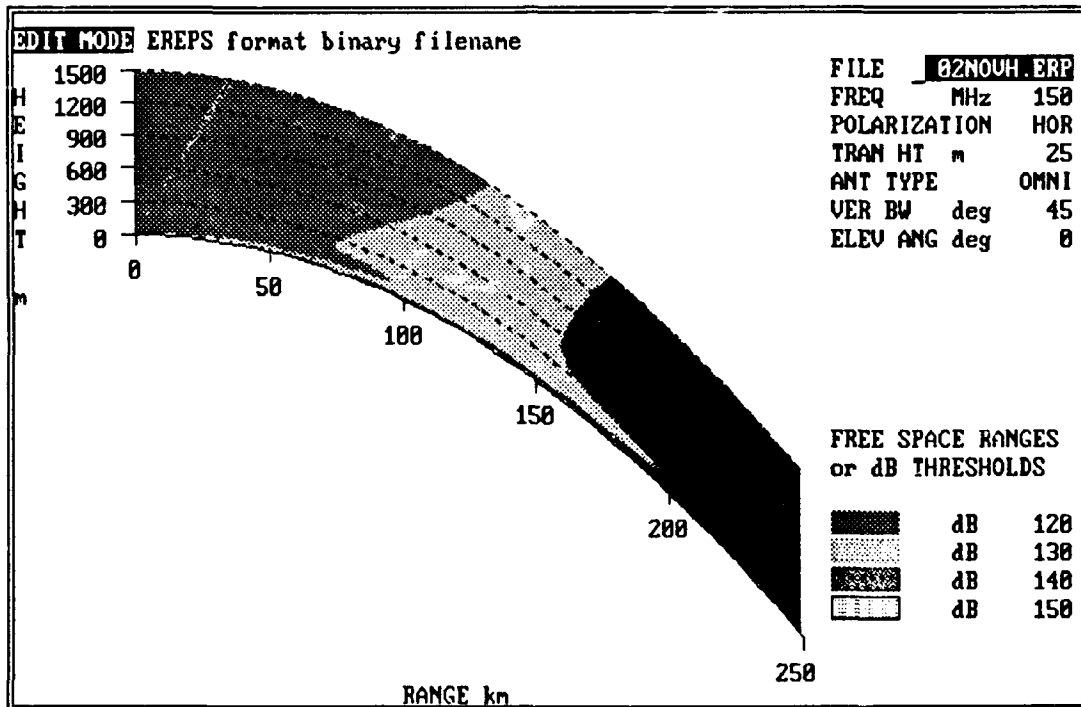


Figure 5.3 RPO homogeneous prediction for 02 NOV 89 (Case 1, 150 MHz)

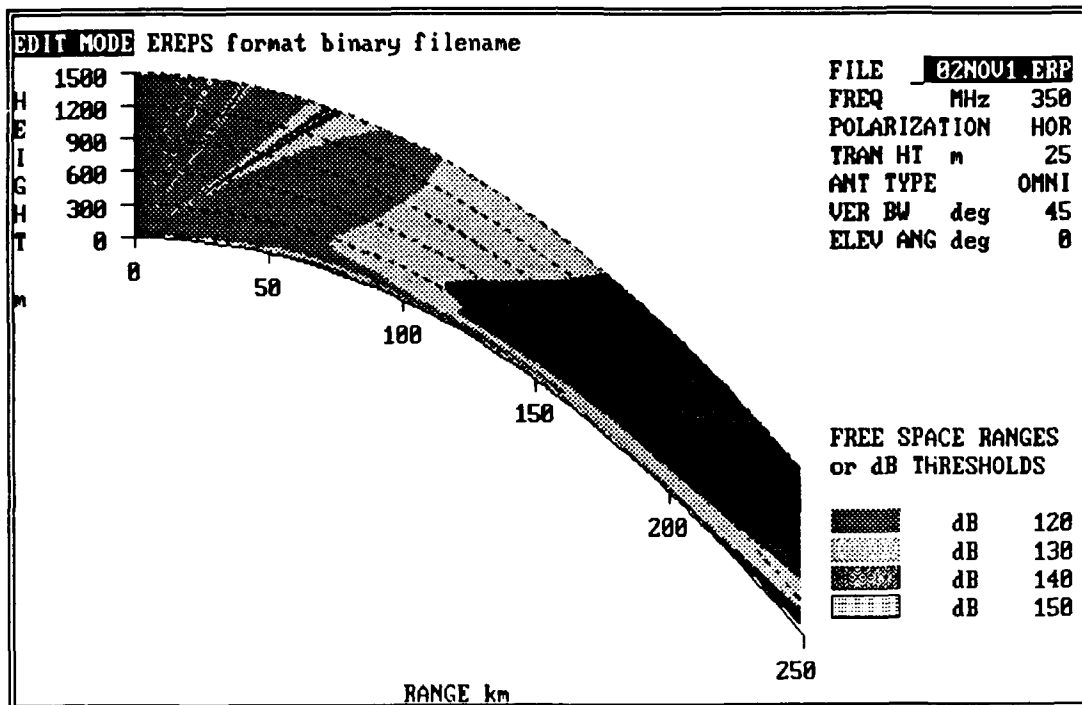


Figure 5.4 RPO inhomogeneous prediction for 02 NOV 89
 (Case 1, 350 MHz)

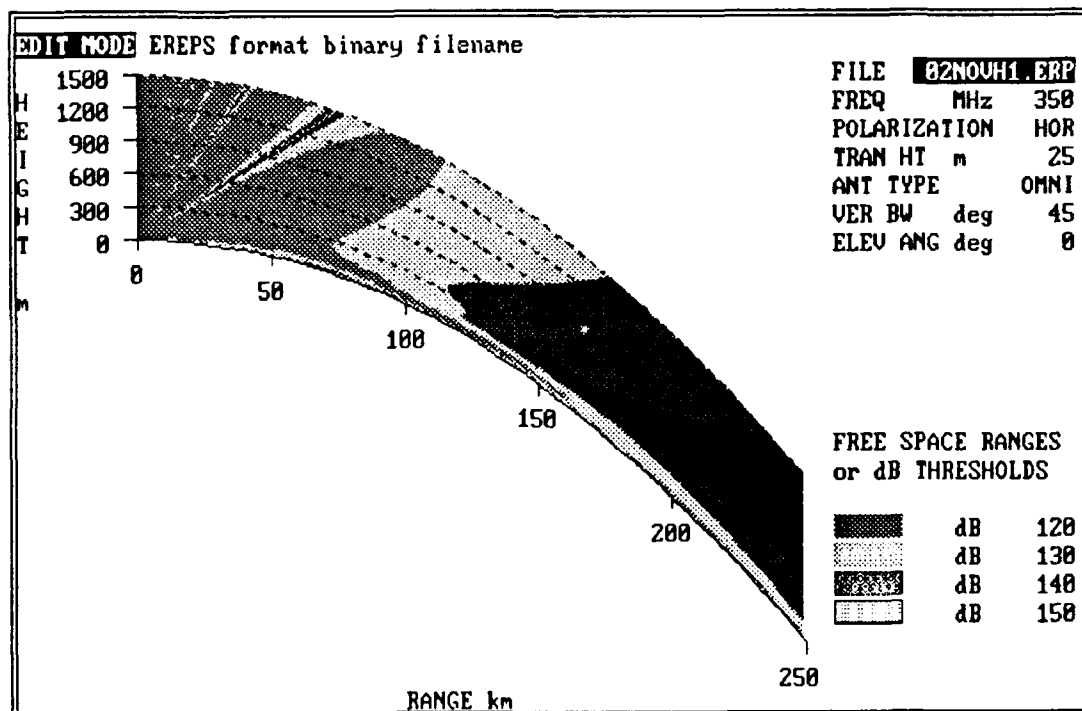


Figure 5.5 RPO homogeneous prediction for 02 NOV 89
 (Case 1, 350 MHz)

signal strength begins to increase in altitude and thickness. Areas of reduced signal strength surround the stronger signal. A region of no detection appears at the surface at approximately 230 kilometers. This behavior, which results from the loss of ducting conditions, is typical beyond the radio horizon. Note that the signal strength over land increases, then decreases, with altitude; at 150 MHz, in contrast, signal strength constantly decreases with height over land.

4. Results for the 3 GHz Analysis

The 3 GHz comparisons are shown in Figures 5.6 and 5.7. As with the previous analysis, the results are identical for the first 180 kilometers. The inhomogeneous prediction shows significant quantitative differences from the homogeneous prediction, notably as lifting, splitting, and widening of the low-threshold duct; these phenomena begin at the 220 kilometer range (just beyond the radio horizon) and become more prominent as the range increases. This again demonstrates that when the duct ceases, normal refraction begins almost immediately. These effects are dramatized by the significantly lower signal strength at this distance from the transmitter. In contrast, the homogeneous prediction illustrates ducting is still in effect, although the signal is developing holes within the duct.

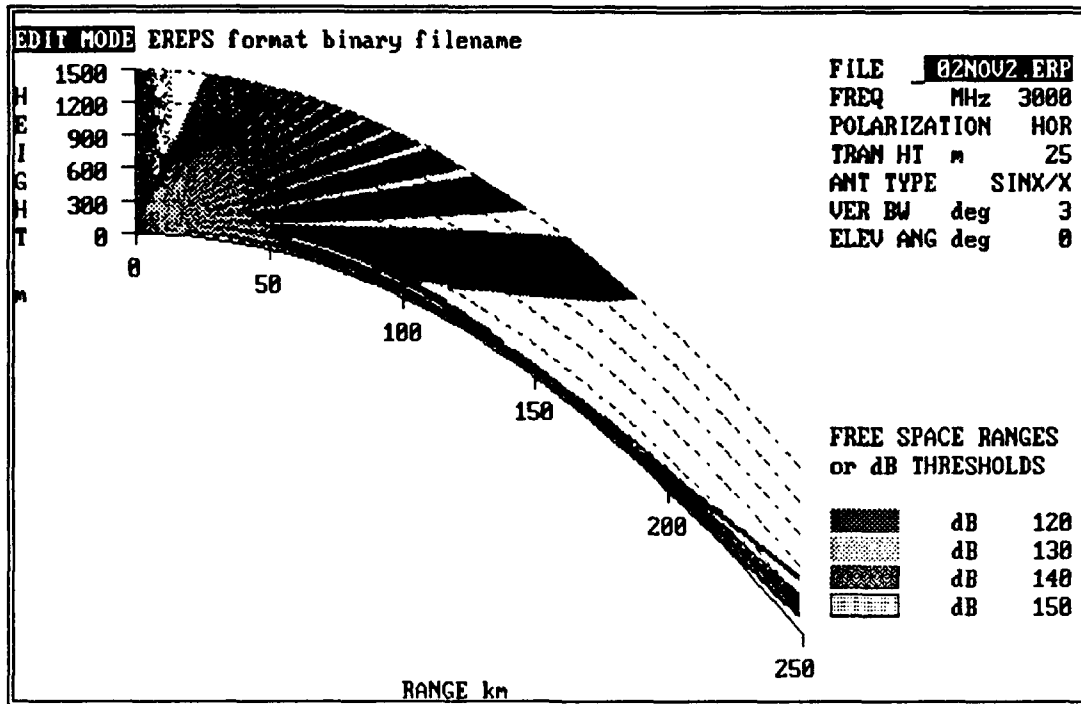


Figure 5.6 RPO inhomogeneous prediction for 02 NOV 89
(Case 1, 3 GHz)

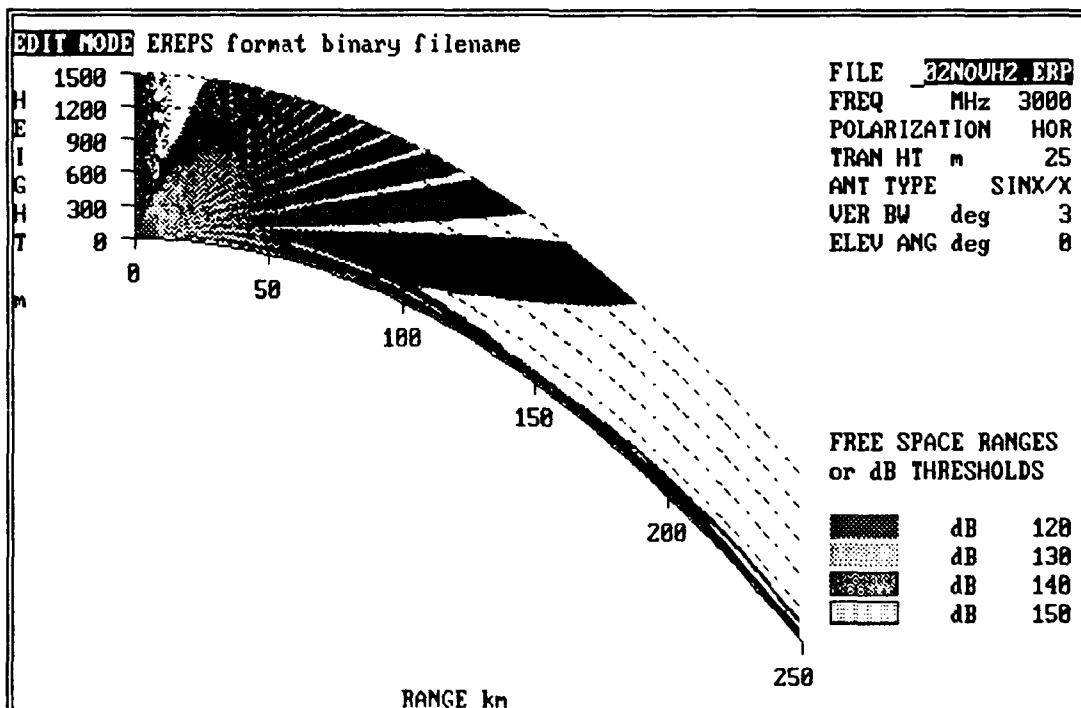


Figure 5.7 RPO homogeneous prediction for 02 NOV 89
(Case 1, 3 GHz)

C. CASE 2

1. Environment

The environmental conditions for Case 2 consist of a surface duct offshore, which is formed by an elevated trapping layer. The over land conditions did not indicate ducting (Figures 3.3 and 3.6).

2. Results for the 150 MHz Analysis

The 150 MHz predictions are shown in Figures 5.8 and 5.9. The homogeneous and inhomogeneous predictions are identical for the first 180 kilometers, after which they diverge. With increasing range, the inhomogeneous atmosphere shows a lifting and widening of the 130 dB duct, with a concomitant reduction of signal strength at the surface. This may be explained by the disappearance of ducting conditions beyond the coastal transition. The homogeneous condition shows a narrowing of the 130 dB duct, with the height decreasing to less than 300 meters at the 250 kilometer range marker. This may be the normal weakening with distance (as $1/R^2$) of the signal outside the duct, with normal duct effect ($1/R$ reduction) inside.

3. Results for the 350 MHz Analysis

The 350 MHz comparisons are shown in Figures 5.10 and 5.11. As for previous cases, these predictions are identical for the first 180 kilometers. At the coastal transition, the ducting conditions begin to disappear and the signal behaves

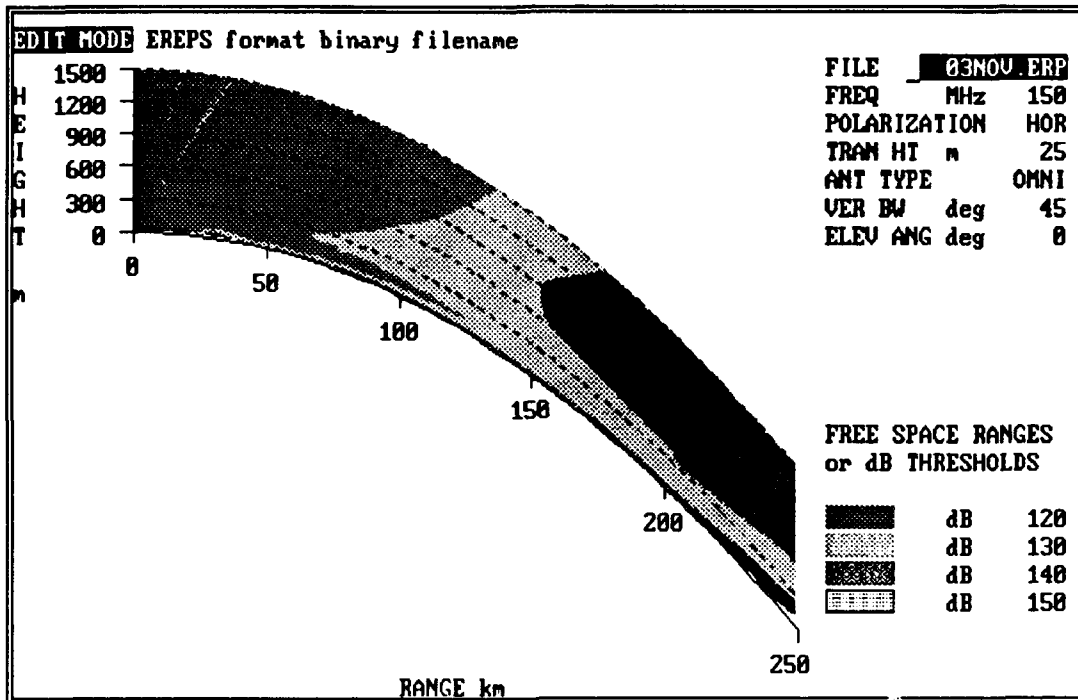


Figure 5.8 RPO inhomogeneous prediction for 03 NOV 89
(Case 2, 150 MHz)

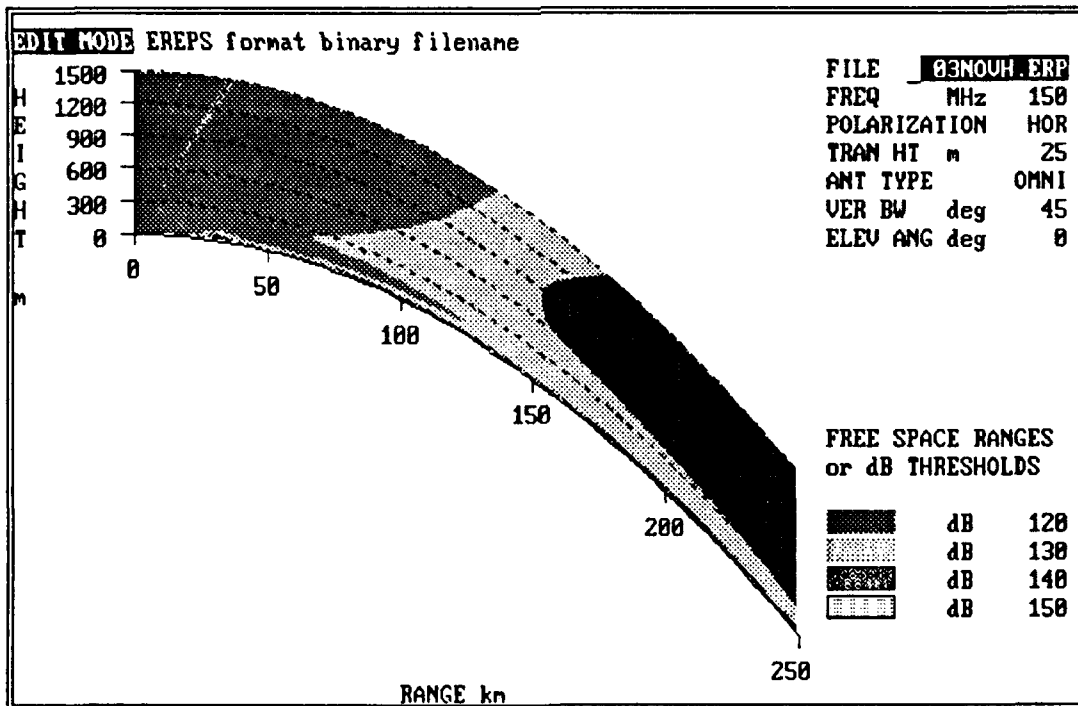


Figure 5.9 RPO homogeneous prediction for 03 NOV 89
(Case 2, 150 MHz)

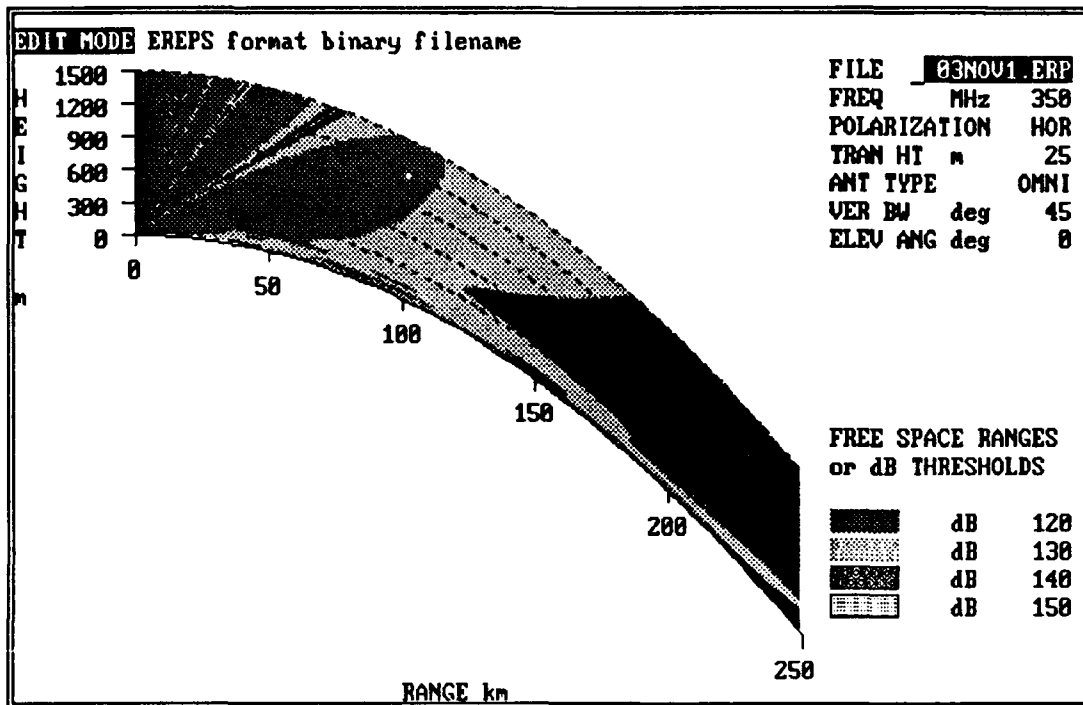


Figure 5.10 RPO inhomogeneous prediction for 03 NOV 89
(Case 2, 350 MHz)

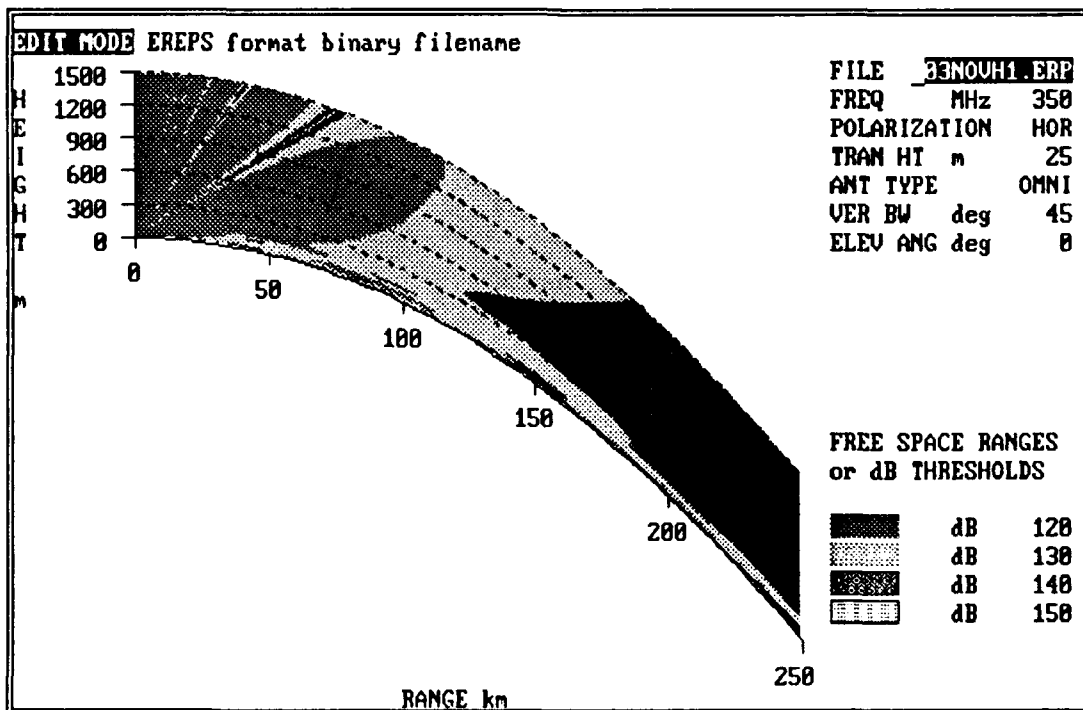


Figure 5.11 RPO homogeneous prediction for 03 NOV 89
(Case 2, 350 MHz)

more typically, with vertical pattern spread and loss of signal beyond the new horizon.

4. Results for the 3 GHz Analysis

The 3 GHz predictions are shown in Figures 5.12 and 5.13. Both predictions are identical offshore until the coastal transition. At this point, several quantitative differences emerge. The inhomogeneous plot shows the maximum signal strength increases with height as distance increases, reaching an altitude of nearly 600 m at the 250 kilometer range marker. In contrast, the homogeneous propagation prediction remains at low altitude (below 150 meters).

5. Interaction Between Duct dM/dz Gradient and Frequency

As described in Chapter IV, the effect of the different types of ducts varies with frequency. This is still noticeable. Case 1, the surface trapping layer, has more channelling effect on UHF frequencies, while the elevated trapping layer of Case 2 has more channelling effect on the VHF frequency.

D. CASE 3

1. Environment

The environmental conditions for Case 3 consists of an elevated duct offshore, with a weak elevated duct over land, as shown in Figures 3.4 and 3.7

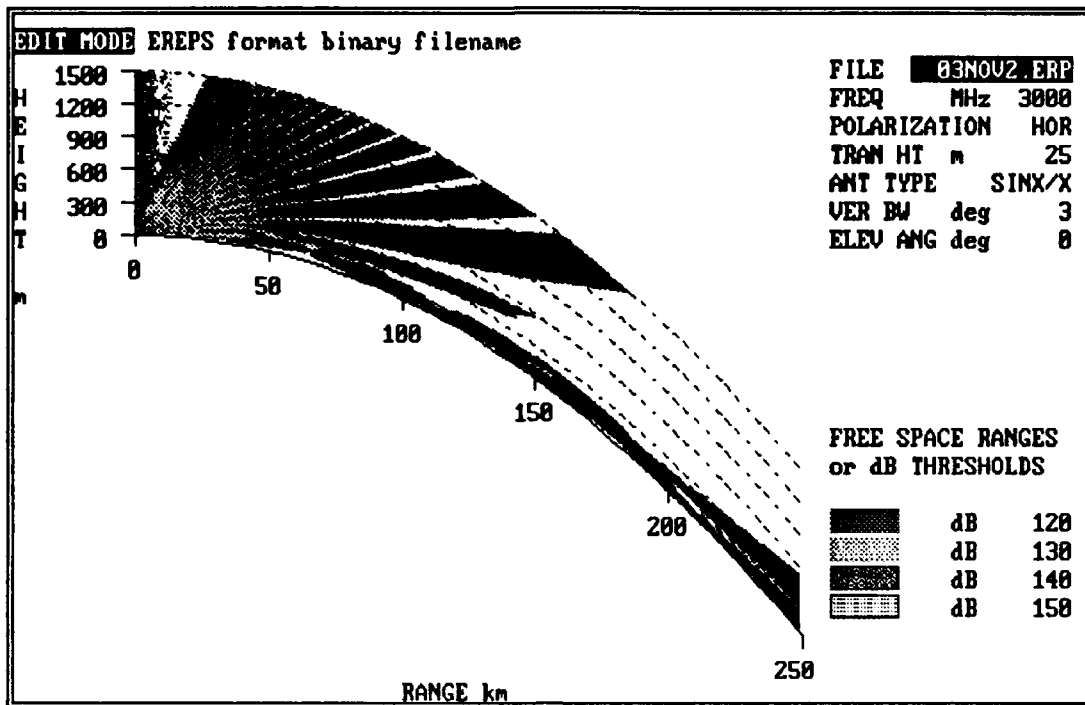


Figure 5.12 RPO inhomogeneous prediction for 03 NOV 89 (Case 2, 3 GHz)

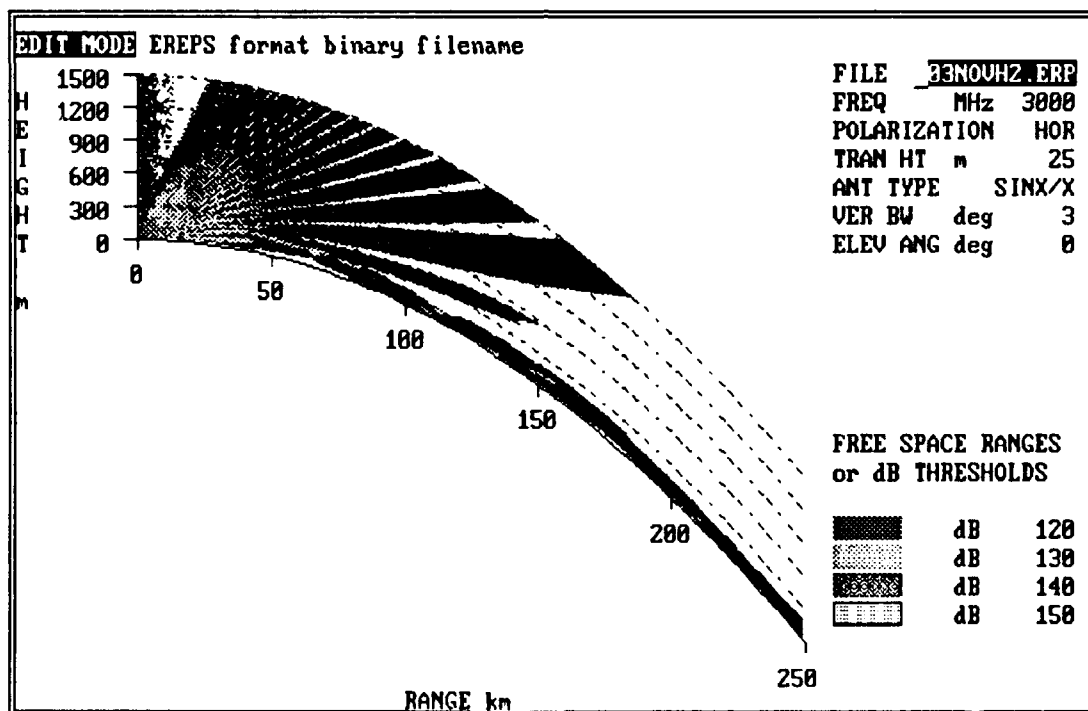


Figure 5.13 RPO homogeneous prediction for 03 NOV 89 (Case 2, 3 GHz)

2. Summarized Results for All Frequencies

No figure comparisons are presented for this case because the inhomogeneous atmosphere predictions are essentially identical to those of the homogeneous atmosphere, which were presented in Chapter IV. The antenna is well below the duct, so there is minimal coupling of energy into the duct for extended propagation. Since the radio horizon occurs well before the inhomogeneous atmospheric region, very little of the signal propagates that far. There is almost no difference between the two predictions. RPO antenna height is currently limited to less than 100 m, which prevents further analysis of the elevated duct.

E. SHORE TO SEA PERSPECTIVE (COASTAL RADAR)

To determine what a coastal early-warning RADAR installation would detect in the same environmental conditions as the battle group, RPO is run using the same M-profiles, but from the opposite direction. Figure 5.14 displays results for Case 1, a surface duct with a surface-based trapping layer. Figure 5.15 presents the predictions for Case 2, a surface duct with an elevated trapping layer.

These trials are only run for a frequency of 3 GHz, which is representative for a coastal RADAR and allows comparison with results for the shipborne RADAR. Case 1 and Case 2 indicate approximately equal detection performance at low altitudes; for both cases the coastal RADAR could detect at

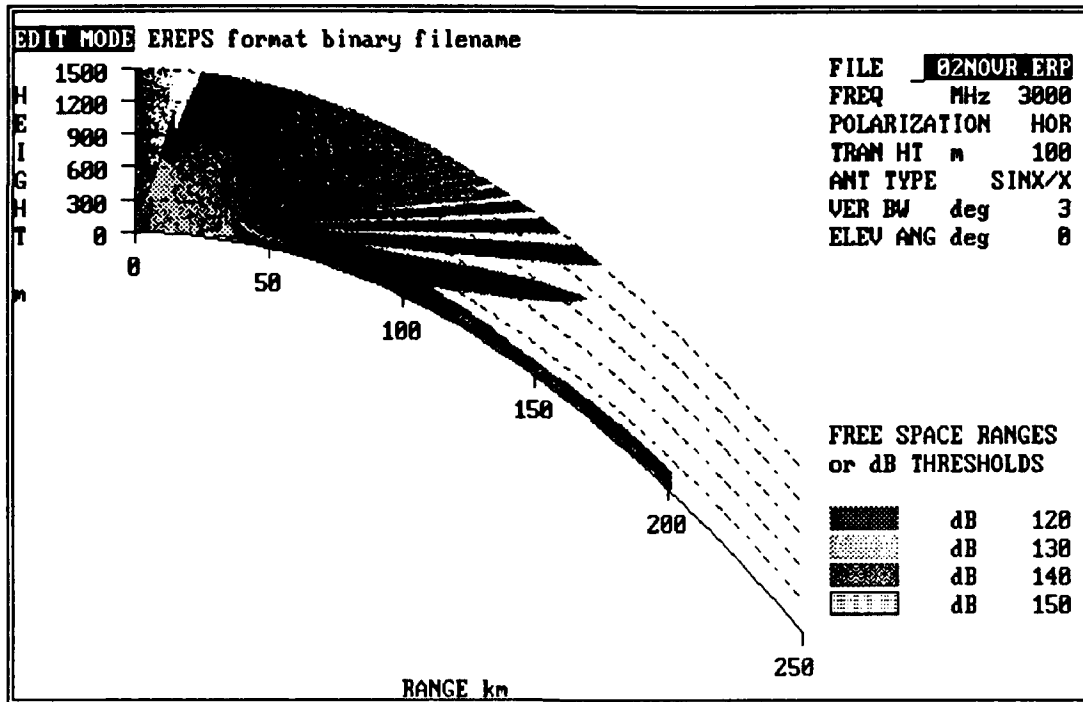


Figure 5.14 Shore to sea prediction for 02 NOV 89
 (Case 1, 3 GHz)

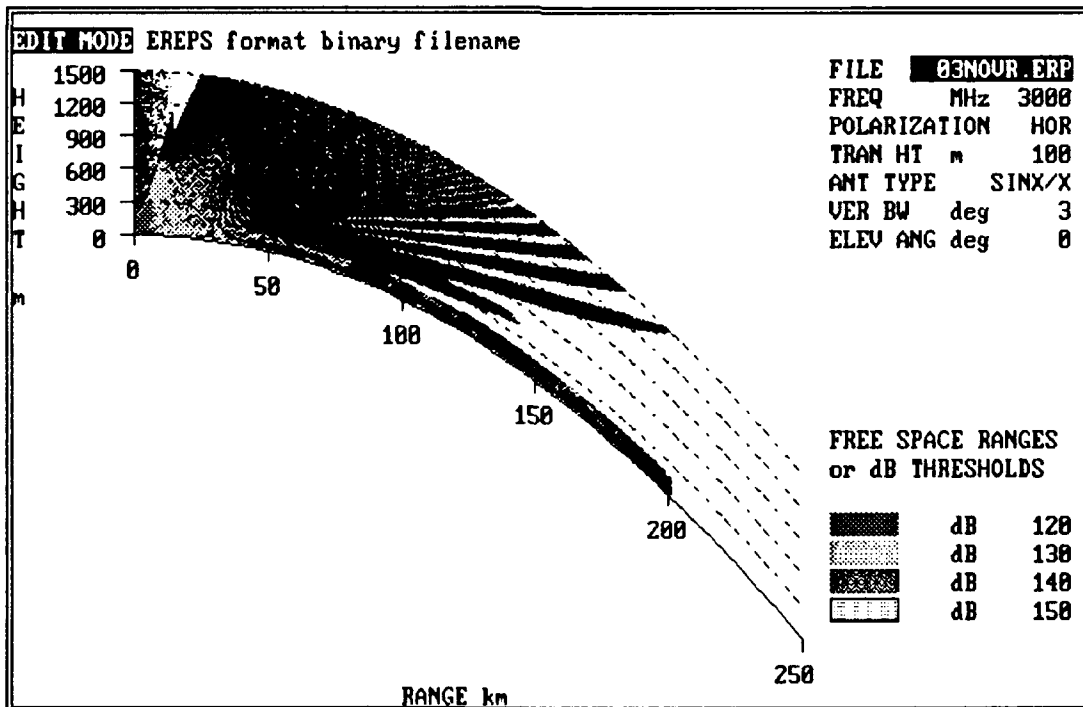


Figure 5.15 Shore to sea prediction for 03 NOV 89
 (Case 2, 3 GHz)

least to the 200 kilometer marker with the same threshold levels. These results indicate that ducting would occur over water, with the expected increased detection range in the duct and coverage holes above the duct. These holes could be exploited for close approach to the shore. The lobe patterns differ somewhat, but not significantly, for these low altitudes.

Comparing these predictions with those from the ship's perspective (Figures 5.7 and 5.13) shows qualitative and quantitative similarities. This is because the RADAR site is located very close to the coastal transition and the offshore duct, so the lack of ducting over land has relatively little influence on the EM propagation.

F. SUMMARY

This chapter compared EM predictions in a horizontally inhomogeneous atmosphere with those in a horizontally homogeneous atmosphere; the atmospheric inhomogeneity results from a coastal transition.

Differences between the homogeneous and inhomogeneous atmosphere predictions begin at the coastal transition. The duct is absent over land, so the offshore channelling effect is lost. Normal spreading of the signal then occurs so signal strength decreases more rapidly with distance. Also, a radio horizon over land develops: the region of highest signal strength begins to increase in altitude and thickness, with

areas of reduced signal strength surrounding the stronger signal, and a region of no detection appears at the surface. This demonstrates that when the duct ceases, normal refraction begins almost immediately.

The predictions for the surface ducts of Case 1 and Case 2 change with frequency, similar to the effect described in Chapter IV: Case 1, with a surface trapping layer, trapped the UHF frequency most strongly, while Case 2, with an elevated trapping layer, trapped the VHF frequency to a greater degree.

These results indicate that considerable prediction error can occur if horizontal homogeneity is erroneously assumed across a coastal transition. When an offshore duct ceases at the coastal transition, detection or communication ranges can be greatly reduced, since normal refraction effects begin almost immediately. With the cessation of the Cold War, the U.S. Navy expects an increase in the requirement for power projection inland; this emphasizes the need for further research to more precisely define and quantify the coastal transition region.

VI. CONCLUSIONS

A. GENERAL

Refractive gradients created by atmospheric variations can significantly alter the propagation path of electromagnetic waves. These atmospheric variations affect the performance of modern electronic weapons systems. The Navy is therefore interested in atmospheric variation and has developed software to predict EM propagation changes through the atmosphere. Such changes are particularly important in coastal zones because of the atmospheric horizontal inhomogeneities in those regions.

The EM prediction software currently used by the Fleet is the Integrated Refractive Index Prediction System (IREPS). For ease and speed of calculation, this model assumes that the atmosphere is horizontally homogeneous, which has been shown to be generally adequate over open water. However, the power projection mission of the Navy requires the Navy to operate near the coast where the land-sea interface affects the atmospheric structure and horizontal homogeneity is no longer a valid assumption. IREPS uses conventional ray tracing techniques to model the atmosphere, neglects signal leakage from ducts, and only approximates the effects of diffraction; these factors severely constrain its performance.

To eliminate many of these deficiencies, the Navy is developing a new prediction system called the Radio Physics Optics (RPO) program. RPO can model horizontal inhomogeneity by using different atmospheric soundings and thus can account for the M-profile variations that occur in the coastal region. Further development might also allow better predictions for elevated ducts. While RPO currently lacks many of the operational features of IREPS, such as the ability to directly input atmospheric data, these could be incorporated in later versions.

RPO includes physics which IREPS omits. RPO is a hybrid which uses parabolic equations for conditions where EM waves are nearly horizontal, which includes duct propagation. The parabolic equations directly compute the effects of leakage, interference, and diffraction. Since IREPS approximates or neglects these factors, it is expected that RPO will model the atmosphere more accurately than IREPS.

B. ASSUMPTIONS IN TESTING

An idealized horizontally inhomogeneous atmospheric structure was assumed for the coastal interface. The offshore profiles represent the atmosphere all the way to a coastal interface of 20 kilometer width, which transitions to a horizontally homogeneous over land profile. This scenario was based on the use of data collected 20 kilometers offshore. The actual coastal transition is probably of larger magnitude,

so these assumptions should underestimate the effect of the coastal transition on propagation.

Since the atmospheric soundings were taken near the middle of the day, the results apply primarily to daytime conditions over land. Neither propagation model can make predictions over rough terrain, so the overland terrain was assumed to be flat and featureless.

This thesis examined three atmospheric conditions: two different surface based ducts offshore, which transition through the coastal interface to non-ducting conditions ashore, and an offshore elevated duct transitioning to a thin, weak elevated duct over land. A plethora of atmospheric conditions are possible. These results only apply to the atmospheric conditions analyzed.

C. PREDICTION DIFFERENCES BETWEEN IREPS AND RPO

RPO's predictions differ markedly from those of IREPS both qualitatively, in the general shape of the propagation patterns, and quantitatively in signal strength as a function of range. The IREPS prediction shows classical ducting, such as extended range and a hole in the coverage in a very idealized fashion. RPO can calculate leakage, diffraction, and interference directly, so it more closely predicts the actual EM propagation pattern and signal strength, and it shows the finer structure of the propagation. RPO predicts smoother transitions to regions of lower signal strength above

the duct, which are termed "leakage". Because of this, signal strength predictions above the duct can differ greatly between the two models. RPO tends to predict shorter propagation ranges within a surface duct than does IREPS, presumably due to leakage leaving less signal remaining to be channelled.

IREPS' wave guide approximation to surface ducts allows no variation in duct thickness as range increases; however, RPO's direct computation of signal strength predicts variations of duct thickness and height at all ranges.

Near the surface of the earth, RPO often predicts a dB loss much greater than that of IREPS; this loss may be caused by diffraction and interference effects, since RPO actually computes both of these effects, whereas IREPS only parameterizes them. This allows RPO to predict where signal strength will vary within the lobes, which IREPS cannot estimate.

Only RPO predicts significant interactions between the duct's dM/dz gradient and frequency: VHF signals propagate farther with an elevated trapping layer, while UHF range is extended with the surface trapping layer. This further illustrates the importance of a direct computation over a parameterizing approximation.

For an elevated duct above the height of the antenna, significant differences between RPO and IREPS predictions are noted only at 150 MHz. The analysis could not be done for an

antenna in the duct because RPO does not guarantee accurate results for an antenna located above 100 meters.

D. RPO RESULTS FOR A HORIZONTALLY INHOMOGENEOUS ATMOSPHERE

RPO can predict EM propagation for a horizontally inhomogeneous atmosphere. The prediction for a horizontally inhomogeneous coastal zone finds significant quantitative differences from the homogeneous prediction. With the disappearance of ducting conditions over land, there is spreading of the signal and the development of a radio horizon. This demonstrates that when the duct ceases, normal refraction begins almost immediately. The coastal transition can have a marked influence on the propagation prediction, which may influence strike tactics.

E. SUMMARY

This thesis has critically compared prediction differences between IREPS and RPO, resulting from RPO's use of more accurate physical techniques. Predictions from the two models do differ significantly under identical atmospheric conditions. The thesis also examined RPO's predictions for a horizontally inhomogeneous coastal transition region. Neglecting this inhomogeneity introduces significant prediction errors.

LIST OF REFERENCES

1. Ko, H. and others, *Anomalous Propagation and Radar Coverage Through Inhomogeneous Atmospheres*, AGARD Conference Proceedings 346, 25, 1984.
2. Patterson, W. L. and others, *IREPS 3.0 Users Manual*, Naval Ocean Systems Center, San Diego, California, September 1987.
3. Patterson, W. L. and others, *Engineer's Refractive Effects Prediction System (EREPS) Revision 2.0*, Naval Ocean Systems Center, San Diego, California, February 1990.
4. Slingsby, P. L., *Tropospheric Propagation Modelling with the Parabolic Equation*, Electronics Research Laboratory, Salisbury, South Australia, September 1990.
5. Culbertson, G.W., *Assessments of Atmospheric Effects on VHF and UHF Communications*, Master's Thesis, Naval Postgraduate School, Monterey, California, March 1990.

BIBLIOGRAPHY

Dockery, G. D., *Modelling Electromagnetic Wave Propagation in the Troposphere Using the Parabolic Equation*, IEEE Transactions on Antennas and Propagation, Volume 36, Number 10, October 1988.

Dotson, M. E., *An Evaluation of the Impact of Variable Temporal and Spatial Data Resolution Upon IREPS*, M.S. Thesis, Naval Postgraduate School, Monterey, California, June 1987.

Ko, H. and others, *An Analysis of EMPE Code Performance in a Selection of Laterally Inhomogeneous Atmospheric-Duct Environments*, Johns Hopkins APL Technical Digest, Volume 9, Number 2, 1988.

Ko, H. and others, *Anomalous Microwave Propagation Through Atmospheric Ducts*, Johns Hopkins APL Technical Digest, Volume 4, Number 1, 1983.

Lee, D. and others, *Finite-Difference Solution to the Parabolic Wave Equation*, J. Acoust. Soc. Am., Volume 68, Number 5, 1981.

Patterson, W. L., *Effective Use of the Electromagnetic Products of TESS and IREPS*, Naval Ocean Systems Center, San Diego, California, October 1988.

Skolnik, M. I., *Introduction to Radar Systems*, McGraw-Hill Book Company, 1962.

INITIAL DISTRIBUTION LIST

1. Defense Technical Information Center 2
Cameron Station
Alexandria, Virginia 22304-6145
2. Library, Code 52 2
Naval Postgraduate School
Monterey, California 93943-5000
3. Director for Command, Control, and 1
Communications Systems, Joint Staff
Washington, DC 20318-6000
4. C3 Academic Group, Code CC 1
Naval Postgraduate School
Monterey, California 93943-5000
5. Professor John W. Glendening, Code MR/GN 1
Naval Postgraduate School
Monterey, California 93943-5000
6. Professor Kenneth L. Davidson, Code MR/OS 1
Naval Postgraduate School
Monterey, California 93943-5000
7. Professor Carlyle H. Wash, Code ME/WX 1
Naval Postgraduate School
Monterey, California 93943-5000
8. Commander 1
NRL Monterey
Naval Postgraduate School
Monterey, California 93943-5000
9. Dr. John Hovermale, Technical Director, Code 212 1
NRL Monterey
Naval Postgraduate School
Monterey, California 93943-5000
10. Mr. G. Love, Code 182 1
NRL Monterey
Naval Postgraduate School
Monterey, California 93943-5000
11. Commander 1
Naval Ocean Systems Center
San Diego, California 92152-5000

- | | | |
|-----|--|---|
| 12. | Dr. J. H. Richter, Code 543 Naval Ocean Systems Center San Diego, California 92152-5000 | 1 |
| 13. | Mr. H. V. Hitney, Code 543 Naval Ocean Systems Center San Diego, California 92152-5000 | 1 |
| 14. | Lt. Bryce Campbell SWOSCOLCOM NETC Newport Newport, Rhode Island 02841 | 1 |
| 15. | Lt. Stephan Siletzky Box 51 Patrol Squadron Special Projects Unit Two NAS Barbers Pt., Hawaii 96862 | 2 |